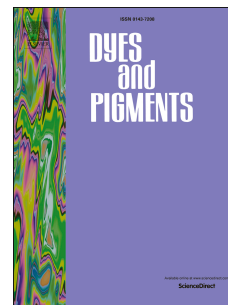


Accepted Manuscript

Methoxy supported, deep red emitting mono, bis and tris triphenylamine-isophorone based styryl colorants: Synthesis, photophysical properties, ICT, TICT emission and viscosity sensitivity

Shantaram Kothavale, Nagaiyan Sekar



PII: S0143-7208(16)30429-6

DOI: [10.1016/j.dyepig.2016.08.025](https://doi.org/10.1016/j.dyepig.2016.08.025)

Reference: DYPI 5405

To appear in: *Dyes and Pigments*

Received Date: 17 June 2016

Revised Date: 8 August 2016

Accepted Date: 9 August 2016

Please cite this article as: Kothavale S, Sekar N, Methoxy supported, deep red emitting mono, bis and tris triphenylamine-isophorone based styryl colorants: Synthesis, photophysical properties, ICT, TICT emission and viscosity sensitivity, *Dyes and Pigments* (2016), doi: 10.1016/j.dyepig.2016.08.025.

This is a PDF file of an unedited manuscript that has been accepted for publication. As a service to our customers we are providing this early version of the manuscript. The manuscript will undergo copyediting, typesetting, and review of the resulting proof before it is published in its final form. Please note that during the production process errors may be discovered which could affect the content, and all legal disclaimers that apply to the journal pertain.

Methoxy supported, deep red emitting mono, bis and tris triphenylamine-isophorone based styryl colorants: Synthesis, Photophysical properties, ICT, TICT emission and viscosity sensitivity

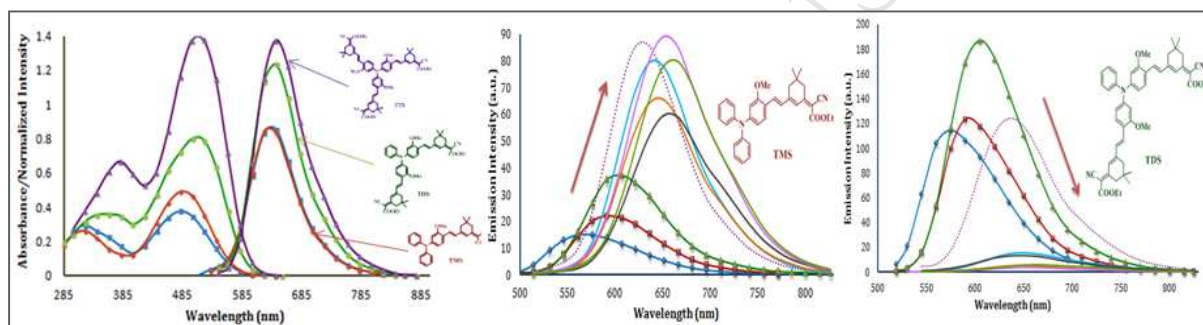
Shantaram Kothavale, Nagaiyan Sekar*

Department of Dyestuff Technology, Institute of Chemical Technology, Matunga,
Mumbai-400 019, India.

E-mail: n.sekar@ictmumbai.edu.in, nethi.sekar@gmail.com

Tel: +91 22 3361 2707; Fax: +91 22 3361 1020.

Graphical abstract



**Methoxy supported, deep red emitting mono, bis and tris triphenylamine-
isophorone based styryl colorants: Synthesis, Photophysical properties, ICT,
TICT emission and viscosity sensitivity**

Shantaram Kothavale, Nagaiyan Sekar*

Department of Dyestuff Technology, Institute of Chemical Technology, Matunga,
Mumbai-400 019, India.

E-mail: n.sekar@ictmumbai.edu.in, nethi.sekar@gmail.com

Tel: +91 22 3361 2707; Fax: +91 22 3361 1020.

Abstract:

A novel strategy for the synthesis of triphenylamine based and methoxy supported deep red emitting push-pull chromophores is developed. The methoxy groups though not in conjugation with the acceptor exhibited a red shifted absorption and emissions (670 nm) as compared to the unsubstituted analogues due to the improved donating ability of triphenylamine. The dyes show high molar extinction coefficients ($1, 65,800 \text{ M}^{-1} \text{ cm}^{-1}$) and as the number of withdrawing groups increases the molar extinction coefficient and emission intensity increase. Positive solvatochromism (96 nm) was observed which is well supported by linear and multi-linear regression. The mono styryl dyes showed enhancement of fluorescence while the di and tri-styryl dyes show quenching of fluorescence in polar solvents, which is correlated with the intramolecular charge transfer and twisted intramolecular charge transfer. Viscosity induced emission enhancement has also been observed. The experimental findings were correlated theoretically by using Density Functional theory computations.

Keywords: Triphenylamine, Push-pull chromophores, Solvatochromism, ICT, TICT, Viscosity sensitivity, Multi-linear regression analysis, and Density Function theory.

1. Introduction:

Triphenylamine, a unique and widely accepted donating group for its very good electron donating ability and charge transfer characteristic has been applied in a number molecules designed for opto-electronic devices. It has been widely used as a framework for the design of two photon absorption (TPA) chromophores[1–7]. The high co-planarity between the central nitrogen atom and the three adjacent carbon atoms makes it possible to maintain uninterrupted conjugation between the lone pair of nitrogen and the dendrimer arms [8–13]. Metal-free organic dyes based on triphenylamine has attracted great attention as the best hole transporting material due to their inexpensive synthesis, high molar extinction coefficient and tunable absorption spectral response [14–19]. Different starburst triarylamine derivatives have been used for their applications in blue to red emitting Organic Light Emitting Diodes (OLEDs) [20–27]. Intramolecular charge transfer (ICT) capability of triphenylamine is also well studied by attaching it with different strong electron accepting group [28–34]. After the debut of the aggregation induced emission (AIE) concept in 2001 initially though the hexaphenyl silol (HPS), tetra-phenyl ethylene (TPE) or plain hydrocarbon based systems were studied for their AIE properties, and recently triphenylamine based donor-acceptor systems are also widely investigated for their very good AIE properties [35–43].

The donating ability of triphenylamine is further increased by attaching supporting/additional donor group at the para position of the two phenyl rings of the

triphenylamine to get improved photophysical properties as well as better efficiency in Dye-sensitized solar cell [44–47]. However after the introduction of the sterically bulky moieties, such as carbazole, diphenylamine, alkoxy substituted phenyl groups and heterocyclic ring as additional donor has increased steric hindrance and further decreased the amount of dye adsorbed on TiO₂ surface in Dye-sensitized solar cell. Therefore to minimize this drawback recently few researchers synthesized and used some methoxy supported triphenylamine derivatives and found very good results where methoxy acts as additional electron donor with triphenylamine as main donor [48]

Though there are number of reports of mono and di-substituted triphenylamine based donor- π -acceptor systems the tri-substituted starburst systems remain as the main attraction recently in the field of Dye-sensitized solar cell due to their better thermal stability, lower aggregation tendency and high molar extinction coefficients [49–52]. The synthesis of such type of starburst derivatives requires very drastic conditions and costly catalysts[1,2,4,5]. We developed a novel synthetic strategy where due to methoxy support the tri-formylation is easily completed by using only up-to 5 equivalent of POCl₃.

Recently fluorescent molecular rotors [FMRs], a group of fluorescent molecules that consists of an electron donor group in π -conjugation with an electron acceptor group and which forms twisted intramolecular charge transfer (TICT) states upon photo excitation have attracted much attention [53–55]. It exhibit two competing de-excitation pathways: fluorescence emission via locally excited state (LE) or via an internal non-radiative process which involves molecular rotation between the donor and the acceptor (TICT). When this rotation is hindered in highly viscous media, the population of the LE state will increase, correspondingly the fluorescence emission intensity will be enhanced [56–58]. Though the 9-dicyanovinyl)-julolidine (DCVJ) and

its different derivatives were extensively studied for their viscosity sensitivity, recently different triphenylamine derivatives also shown to have very good FMR properties due to the freely rotating phenyl rings around C-N bond which gets hindered in viscous environment causing fluorescence enhancement [59]. In general the TICT states are dark states causing quenching of fluorescence in polar solvents, which further becomes emissive in a highly viscous environment. Among the four dyes we studied i.e. mono-methoxy mono-styryl dye (**TMS**), tri-methoxy mono-styryl dye (**TTMS**), di-methoxy di-styryl dye (**TDS**) and tri-methoxy tri-styryl dye (**TTS**), we found quenching of fluorescence for **TDS** and **TTS**, due to the TICT state while enhancement of fluorescence for **TMS** and **TTMS** in polar solvents may be due to the simply ICT state. When we studied these dyes for their viscosity effect, as expected we found better enhancement of fluorescence for **TDS** and **TTS** dye as compared to **TMS** and **TTMS** dyes.

<< **Please insert Fig. 1. Structures of the synthesized dyes TMS, TTMS, TDS and TTS** >>

The methoxy supported dyes showed red shifted absorption as well as emission as compared to the known triphenylamine styryl dyes from our group [60] as well as isophorone based extended styryl dyes [61]. All these dyes are fluorescent in solution as well as in solid state. Solvatochromism study of all these dyes were carried out in non-polar to polar solvents. Density functional theory computations [B3LYP/6-31G (d)] were used to study the geometrical and electronic properties of the synthesized molecules.

2. Experimental section

2.1 Materials and equipments

All the reagents and solvents required for the synthesis were purchased from S d Fine Chemical Limited, Mumbai, India and used without further purification. The reactions were monitored by TLC using on 0.25 mm E-Merck silica gel 60 F254 precoated plates, which were visualized with UV light. ^1H (500 MHz) and ^{13}C (125 MHz) NMR spectra were recorded on a Varian Cary Eclipse Australia. The chemical shift values are expressed in δ ppm using CDCl_3 and DMSO-d_6 as solvents and TMS (Tetramethylsilane) as an internal standard. High resolution liquid chromatography mass spectra were recorded on 6550 iFunnel QTOF LC/MS spectrometer from Agilent Technologies. Melting points were measured on standard melting point apparatus from Sunder Industrial Product Mumbai and are uncorrected. The absorption spectra of the compounds were recorded on a PerkinElmer UV- visible spectrophotometer Lambda 25. Fluorescence emission spectra were recorded on Varian Cary Eclipse fluorescence spectrophotometer using freshly prepared solutions at the concentration of 1×10^{-6} mol L^{-1} . Fluorescence quantum yields were determined in different solvents by using Rhodamine B ($\Phi = 0.97$ in ethanol) as a reference standard using the comparative method.

2.2 Computational Methods

Density Functional Theory (DFT) [62] was used to optimize ground state (S_0) geometry of all compounds by using the Gaussian 09 package and the popular hybrid functional B3LYP. The B3LYP combines Becke's three parameter exchange functional (B3)[63] with the nonlocal correlation functional by Lee, Yang, and Parr (LYP) [64]. The basis set used for all atoms was 6-31G (d) in both DFT and time-dependent density functional theory (TD-DFT) method. The low-lying first singlet excited states (S_1) of the dyes were relaxed to obtain their minimum energy geometries using the TD-DFT in their gas phase. By using TD-DFT at the same hybrid

functional and basis set, the vertical excitation energies and oscillator strengths were obtained for the lowest 20 singlet-singlet transitions at the optimized ground state equilibrium geometries [65]. Frequency computations were also carried out on the optimized geometry of the low-lying vibronically relaxed first excited state of conformers. Optimized ground state structures were utilized to obtain the electronic absorption spectra, including maximum absorption and oscillator strengths.

2.3 Synthetic strategy

To check out the effect of extra number of additional methoxy groups as well as withdrawing isophorone ester groups on main triphenylamine donor moiety four different D- π -A styryl derivatives were successfully synthesized. A novel and easy synthetic route has been developed to get the mono, di and tri-formylated triphenylamine intermediates (6, 7, and 8). Mono-methoxy substituted intermediate 3 was successfully synthesized by Buchwald coupling reaction starting from 3-methoxy aniline and iodobenzene using 1, 10 phenanthroline and CuI as catalyst. For the synthesis of intermediate 4 and 5, we utilized 3-bromo anisole as reagent instead of iodobenzene for additional methoxy groups, using the same Buchwald coupling reaction condition and refluxing the reaction mixture for extra time (48 h). The Buchwald coupling reaction of 3-bromo anisole with 3-methoxy aniline was giving better yield as compared to that of aniline as a starting compound.

The formylated intermediate 6 and 9 were synthesized by using regular Vilsmeiere-Haack formylation at room temperature, and a little harsh reaction condition was required for the synthesis of intermediate 7 and 8. Initially after generating the Vilsmeiere-Haack adduct at room

temperature, the methoxy intermediate were dissolved in 1, 2 dichloroethane and added drop wise to the reaction mixture and then refluxed for 12 h to get the desired formylated product (Figure S15). Little excess POCl₃ and extra time was given for the synthesis of intermediate 8. Both the derivatives were purified on column chromatography (100-200 mesh size silica). Final styryl derivatives (**TMS**, **TDS** and **TTMS**) were obtained by using regular Knoevenagel condensation reaction condition (i.e. Piperidine/ethanol) to get the pure products after filtration, while styryl derivative **TTS** was synthesized by refluxing the reaction mixture for 12 h in acetonitrile and piperidine as catalyst, crude product obtained after filtration was purified by column chromatography.(100-200 mesh size silica).

<< **Please insert Scheme 1. Synthesis of TMS, TDS, TTS and TTMS** (a) Iodobenzene, potassium-t-butoxide,1,10 Phenanthroline / CuI, toluene (b)3-bromo anisole, potassium-t-butoxide,1,10 Phen / CuI, toluene (c) DMF/POCl₃ (d) DMF/POCl₃, 1,2 dichloroethane (e)1,1-piperidine,ethanol (f) ethyl cyanoacetate, NH₄OAc, acetic acid, toluene. >>

2.4 Synthesis and characterization

2.4.1 Synthesis of 3-methoxy-N, N-diphenylaniline (3)

To a stirred solution of m-anisidine (20 g, 162.4 mmol), iodobenzene (39.8 ml, 357.28 mmol), and 1,10 phenanthroline (1.17 g, 6.49 mmol) in toluene (350 ml) were added potassium t-butoxide (54 g, 112.21 mmol) and copper(I) iodide (1.23 g, 6.49 mmol). The reaction mixture was heated under reflux for 24 h at 125 °C. On completion of the reaction, the mixture was cooled to room temperature, and filtered to remove copper metal. The filtrate was extracted by

adding more ethyl acetate. The combined organic phases were concentrated under vacuum and purified by column chromatography using 5 % EtOAc in hexane as the eluent to get the pure product (colorless oil) (29.5 g, 66.08 %) ^1H NMR (500 MHz, CDCl_3): δ 7.24 (t, $J = 7.9$ Hz, 4H), 7.14 (t, $J = 8.5$ Hz, 1H), 7.09 (d, $J = 7.9$ Hz, 4H), 7.01 (d, $J = 7.3$ Hz, 2H), 6.65 (d, $J = 8.5$ Hz, 1H), 6.62 (s, 1H), 6.56 (d, $J = 8.5$ Hz, 1H), 3.71 (s, 3H); ^{13}C NMR (125 MHz, CDCl_3): δ 160.4, 149.1, 147.7, 129.8, 129.2, 124.4, 122.8, 116.4, 109.7, 107.9, 55.2 ppm.

2.4.2 Synthesis of 3-methoxy-N-(3-methoxyphenyl)-N-phenyl aniline (4)

To a stirred solution of aniline (30 g, 322.13 mmol), 3-bromo anisole (93 ml, 740.89 mmol), and 1,10 phenanthroline (2.32 g, 12.88 mmol) in toluene (300 ml) were added potassium-t-butoxide (108.4 g, 966.39 mmol) and copper(I)iodide (2.45 g, 12.88 mmol). The mixture was heated under reflux for 48 hrs at 130°C under nitrogen atmosphere. The starting material and intermediate (3-methoxy-N-phenylaniline) formed during reaction were not getting fully converted into the product even after adding excess potassium-t-butoxide (18.07 g, 161.065 mmol) and 3-bromo anisole (20.21 ml, 161.065 mmol). The reaction mixture was cooled to room temperature, filtered to remove copper metal. The filtrate was extracted by adding more ethyl acetate (200 ml x 3). The combined organic phases were concentrated under vacuum and purified by column chromatography using 5 % EtOAc in hexane as the eluent to get the pure product (colorless oil). (24.5 g, 24.90 %) ^1H NMR (500 MHz, CDCl_3): δ 6.99-7.22 (m, 7H), 6.61-6.65 (m, 4H), 6.53-6.55 (d, $J = 8$ Hz, 2H), 3.69 (s, 6H); ^{13}C NMR (125 MHz, CDCl_3): δ 160.32, 148.87, 147.49, 129.65, 129.08, 124.53, 122.89, 116.61, 109.93, 108.07, 55.14 ppm.

2.4.3 Synthesis of tris (3-methoxyphenyl) amine (5)

To a stirred solution of m-anisidine (30 g, 243.60 mmol), 3-bromo anisole (91.73 ml, 730.81 mmol), and 1,10 phenanthroline (1.75 g, 9.74 mmol) in toluene (300 ml) were added potassium-t-butoxide (82 g, 730.81 mmol) and copper(I)iodide (1.85 g, 9.74 mmol). The mixture was heated under reflux for 48 h at 130 ° C under nitrogen atmosphere. The starting material and intermediate (bis(3-methoxyphenyl)amine) formed during reaction was not getting fully converted into the product even after the addition of excess potassium-t-butoxide (13.66 g, 121.8 mmol) and 3-bromo anisole (15.28 ml, 161.065 mmol). The reaction mixture was cooled to room temperature, filtered to remove copper metal. The filtrate was extracted by adding more ethyl acetate (200 ml x 3). The combined organic phases were concentrated under vacuum and purified by column chromatography using 2 % EtOAc in hexane as the eluent to get the pure product (colorless oil). (31 g, 37.94 %) ¹H NMR (500 MHz, CDCl₃): δ 7.14-7.17 (t, J = 8 Hz, 3H), 6.66-6.70 (m, 6H), 6.57-6.59 (dd, J = 8 and 2.5 Hz, 3H), 3.73 (s, 9H); ¹³C NMR (125 MHz, CDCl₃): δ 160.38, 148.80, 129.75, 116.92, 110.21, 108.33, 55.24 ppm.

2.4.4 Synthesis of 4-(diphenylamino)-2-methoxybenzaldehyde (6)

POCl₃ (2.54 ml, 27.23 mmol) was added drop-wise into ice-cooled N,N-dimethyl formamide (7 ml, 90.79 mmol) at 0 ° C under nitrogen atmosphere and the mixture was stirred at room temperature for an hour. The Vilsmeier adduct formed was again cooled to 0 ° C, compound 3 (5 g, 18.15 mmol) dissolved in DMF was added drop-wise and the mixture was stirred at 50 ° C for 1 hr. On cooling water was added to the reaction mixture, the yellow colored solid precipitated out was filtered and dried well as pure product. (4.6 g, 83.48 %, melting point=128 ° C) ¹H NMR (500 MHz, CDCl₃) δ 3.69 (s, 3H), 6.45 (d, J=1.5, 1H), 6.52-6.54 (dd, J=8.5 and 2, 1H), 7.16-7.19 (m, 6H) 7.33-7.36 (t, 4H), 7.65-7.67 (dd, J=9 and 0.5, 1H), 10.23 (s, 1H). ¹³C NMR

(125 MHz, CDCl₃) 55.39, 101.74, 112.22, 118.21, 125.15, 126.44, 129.64, 129.88, 146.13, 154.84, 163.09, 187.79.

2.4.5 Synthesis of 4,4'-(phenylazanediyl)bis(2-methoxybenzaldehyde)(7)

POCl₃ (7.65 ml, 81.86 mmol) was added drop-wise into ice-cooled N,N-dimethyl formamide (12.71 ml, 163.73 mmol) at 0 ° C under nitrogen atmosphere and the mixture was stirred at room temperature for an hour. The Vilsmeier adduct formed was again cooled up-to 10 ° C, compound 4 (5 g, 16.373 mmol) dissolved in 1, 2 dichloroethane (50 ml) was added drop-wise and the mixture was stirred at 80 ° C for 5-6 hrs. On cooling to room temperature water was added in the reaction mixture and extracted with DCM (100 x 3 ml). The combined organic phases were concentrated under vacuum and purified by column chromatography using 1 % MeOH in DCM as the eluent to get the pure product. (4.3 g, 72.75 %, melting point=148 ° C).

¹H NMR (500 MHz, CDCl₃) δ 3.74 (s, 6H), 6.62-6.63 (d, J = 2, 2H), 6.67-6.70 (dd, J = 8.5 and 2, 2H) 7.17 -7.19 (m, 2H), 7.24-7.27 (m, 1H), 7.37- 7.40 (m, 2H), 7.72- 7.74 (d, J = 8.5, 2H), 10.30 (s, 2H). ¹³C NMR (125 MHz, CDCl₃): δ 55.57, 105.54, 115.46, 120.27, 126.25, 127.05, 129.89, 129.97, 145.33, 153.36, 162.88, 188.06.

2.4.6 Synthesis of 4, 4', 4''-nitrilotris (2-methoxybenzaldehyde) (8)

POCl₃ (13.93 ml, 149.07 mmol) was added drop-wise into ice-cooled N,N dimethyl-formamide (23.18 ml, 298.15 mmol) at 0 ° C under nitrogen atmosphere and the mixture was stirred at room temperature for an hour. To this adduct compound 5 (10 g, 29.8 mmol) dissolved in 1.2 dichloroethane (100 ml) was added drop-wise and the mixture was stirred at 90 ° C for 12 hrs. On cooling to room temperature water was added in the reaction mixture and extracted with

DCM (150 x 3 ml). The combined organic phases were concentrated under vacuum and purified by column chromatography using 2 % MeOH in DCM as the eluent to get the pure product. (7.6 g, 60.8 %, melting point=231 ° C).

¹H NMR (500 MHz, CDCl₃) δ 3.79 (s, 9H), 6.68-6.69 (d, J = 2, 3H), 6.74-6.76 (dd, J = 8.5 and 1.5, 3H), 7.78-7.80 (d, J = 8.5, 3H), 10.35 (s, 3H). ¹³C NMR (125 MHz, CDCl₃): δ 55.70, 107.28, 116.97, 121.19, 129.81, 152.37, 162.78, 188.12.

2.4.7 Synthesis of 4-(bis (3-methoxyphenyl) amino)-2-methoxybenzaldehyde (9)

POCl₃ (0.72 ml, 7.75 mmol) was added drop-wise into ice-cooled N,N dimethyl formamide (2.31 ml, 29.83 mmol) at 0 ° C under nitrogen atmosphere and the mixture was stirred at room temperature for an hour. The Vilsmeier adduct thus formed was again cooled to 0 ° C, compound 5 (2 g, 5.96 mmol) dissolved in DMF (10 ml) was added drop-wise and the mixture was stirred at room temperature for 1 hr. On cooling to 10 ° C, ice-water was added in the reaction mixture; the solid precipitated out was filtered and dried well as pure product. (1.8 g, 83.33 %, melting point =143° C)

¹H NMR (500 MHz, CDCl₃) δ 3.72 (s, 3H), 3.76 (s, 6H), 6.49 (d, J = 1.5, 1H), 6.54-6.56 (dd, J = 8.5 and 2, 1H), 6.71-6.73 (m, 4H), 6.76-6.78 (m, 2H), 7.23-7.26 (m, 2H), 7.65-7.67 (d, J=8.5, 1H), 10.23 (s, 1H). ¹³C NMR (125 MHz, CDCl₃): δ 55.34, 55.46, 102.23, 110.66, 112.19, 112.68, 118.37, 118.71, 129.79, 130.21, 147.14, 154.60, 160.64, 163.02, 187.87.

2.4.8 Synthesis of (Z)-ethyl 2-cyano-2-(3-((E)-4-(diphenylamino)-2-methoxystyryl)-5, 5-dimethylcyclohex-2-en-1-ylidene) acetate (TMS)

Compound 6 (0.3 g, 0.98 mmol) and compound 11 (0.34 g, 1.48 mmol) were dissolved in absolute ethanol, 1-2 drops of piperidine was added and the mixture was refluxed for 2 hrs. After

cooling to room temperature the dark red colored solid separated out was filtered, washed with small quantity of absolute ethanol and dried well to get the pure product. (0.4 g, 78.43 %, melting point = 222 ° C)

¹H NMR (500 MHz, CDCl₃) δ 1.03 (s, 6H), 1.33-1.36 (t, 3H), 1.59 (s, 2H), 2.97 (s, 2H), 3.69 (s, 3H) 4.23-4.28 (q, 2H), 6.55 (d, J = 2, 1H), 6.58-6.59 (d, J = 2.5, 1H), 6.60-6.61 (s, J = 2.5, 1H), 6.86 (s, 1H), 6.95 (s, 1H), 6.98 (s, 1H), 7.06-7.14 (m, 5H), 7.25-7.30 (m, 4H). 7.37-7.39 (d, J = 8.5, 1H). ¹³C NMR (126 MHz, CDCl₃): δ 14.18, 28.36, 30.89, 31.41, 38.80, 41.01, 55.45, 61.21, 98.16, 104.77, 114.86, 116.94, 118.68, 123.88, 125.34, 127.95, 128.07, 129.37, 129.82, 146.93, 150.17, 153.75, 158.41, 163.44, 167.01, 206.87. HRMS (ESI): m/z calculated for (M + H)⁺ C₃₄H₃₄N₂O₃, 519.2569; found 519.2592.

2.4.9 Synthesis of (2Z,2'Z)-diethyl 2,2'-(((1E,1'E)-((phenylazanediy)bis(2-methoxy-4,1-phenylene))bis(ethene-2,1-diyl))bis(5,5-dimethylcyclohex-2-en-3-yl-1-ylidene))bis(2-cyanoacetate)(TDS)

Compound 7 (0.4 g, 1.10 mmol), compound 11 (0.77 g, 3.32 mmol) and 1-2 drop piperidine were refluxed in anhydrous acetonitrile for 6 hr under nitrogen atmosphere. On cooling to room temperature the dark red colored solid separated was filtered and dried well to get the pure product (0.44 g, 50.57 %, melting point=188-192 ° C)

¹H NMR (500 MHz, CDCl₃) δ 0.96 (s, 6H), 0.99 (s, 6H), 1.23-1.26 (t, 6H), 2.42 (s, 2H), 2.43 (s, 2H), 2.57 (s, 2H), 2.91 (s, 2H), 3.67 (s, 6H) 4.16-4.22 (q, 4H), 6.52-6.55 (dd, J = 8.5 and 2, 2H), 6.65-6.66 (d, J = 2, 2H), 6.79 (s, 1H), 7.06-7.09 (d, J = 16, 1H), 7.14-7.20 (m, 4H), 7.26-7.30 (m, 2H), 7.37-7.40 (t, J = 8, 2H) 7.67-7.68 (d, J = 9, 1H), 7.70-7.72 (d, J = 9, 1H), 7.78 (s, 1H). ¹³C NMR (126 MHz, CDCl₃) δ 14.49, 28.07, 28.28, 31.51, 31.96, 38.34, 38.77, 40.93, 44.59, 56.03,

61.53, 97.25, 97.94, 106.20, 116.07, 116.79, 117.58, 119.81, 123.24, 125.03, 125.50, 126.38, 146.14, 149.20, 153.99, 154.61, 158.45, 162.53, 162.97, 165.40, 167.07. HRMS (ESI): m/z calculated for (M + H)⁺ C₅₀H₅₃N₃O₆, 792.3934; found 815.3971(+Na).

2.4.10 Synthesis of (2Z,2'Z,2''E)-triethyl 2,2',2''-(((1E,1'E,1''E)-(nitrilotris(2-methoxybenzene-4,1-diyl))tris(ethene-2,1-diyl))tris(5,5-dimethylcyclohex-2-en-3-yl-1-ylidene))tris(2-cyanoacetate)(TTS)

Compound 8 (0.3 g, 0.71 mmol), compound 11 (0.83 g, 3.57 mmol) and 1-2 drop piperidine were refluxed in anhydrous acetonitrile for 12 h under nitrogen atmosphere. On cooling to room temperature the dark red colored solid separated was filtered, dried and purified by column chromatography (10 % EtOAc in hexane) to get the pure product (0.22 g, 28.94%, melting point= 158-162 ° C)

¹H NMR (500 MHz, CDCl₃) δ 0.96 (s, 9H), 0.99 (s, 9H), 1.22-1.26 (t, 9H), 2.42 (s, 3H), 2.43 (s, 3H), 2.57 (s, 3H), 2.91 (s, 3H), 3.70 (s, 9H) 4.16-4.22 (q, 6H), 6.62-6.64 (d, J = 8.5, 3H), 6.73 (d, J = 1, 3H), 6.80 (s, 1H), 7.09-7.12 (d, J = 16.5, 2H), 7.20-7.32 (m, 4H), 7.70-7.80 (m, 5H). ¹³C NMR (126 MHz, CDCl₃): δ 14.49, 28.06, 28.27, 31.12, 31.51, 31.93, 38.33, 38.76, 40.93, 44.57, 56.16, 61.55, 97.47, 98.13, 107.34, 116.65, 117.16, 117.53, 120.72, 123.76, 125.27, 128.85, 129.41, 129.82. HRMS (ESI): m/z calculated for (M + H)⁺ C₆₆H₇₂N₄O₉, 1065.5299; found 1065.5283.

2.4.11 Synthesis of (Z)-ethyl 2-(3-((E)-4-(bis (3-methoxyphenyl) amino)-2-methoxystyryl)-5, 5-dimethylcyclohex-2-en-1-ylidene)-2-cyanoacetate (TTMS)

Compound 9 (0.3 g, 0.82 mmol), compound 11 (0.28 g, 1.23 mmol) and 1-2 drop piperidine were refluxed in absolute ethanol for 12 h, 1 h under nitrogen atmosphere. On cooling to room

temperature the solid separated was filtered and dried and purified by column chromatography (15 % EtOAc in hexane) to get the pure product (0.16 g, 33.54 %, melting point = 123 ° C)

^1H NMR (500 MHz, DMSO- d_6) δ 0.97 (s, 3H), 1.00 (s, 3H), 1.22-1.26 (t, 3H), 2.42-2.44 (d, 2H), 2.57 (s, 1H), 2.92 (s, 1H), 3.68 (s, 9H), 4.18-4.22 (q, 2H), 6.46-6.47 (d, 1H), 6.56-6.76 (m, 9H), 7.24-7.31 (m, 3H), 7.62-7.68 (dd, 1H). ^{13}C NMR (126 MHz, dmsO- d_6) δ 14.51, 28.08, 28.29, 31.52, 31.93, 55.60, 55.93, 61.51, 97.05, 97.70, 101.27, 104.86, 110.14, 111.29, 111.73, 112.71, 114.84, 116.85, 117.86, 118.77, 119.20, 123.00, 124.76, 128.34, 128.63, 128.75, 129.99, 130.28, 130.82, 131.12, 146.85, 147.85, 149.82, 154.78, 158.47, 160.64, 160.80, 162.58, 163.02, 165.45, 167.13, 186.88. HRMS (ESI): m/z calculated for $(\text{M} + \text{H})^+$ $\text{C}_{36}\text{H}_{38}\text{N}_2\text{O}_5$, 579.2781; found 579.2802.

2.4.12 Synthesis of (Z)-ethyl 2-cyano-2-(3, 5, 5-trimethylcyclohex-2-en-1-ylidene) acetate (11)

Synthesized by using the reported literature procedure [66]

Isophorone (10 g, 72.35 mmol) and ethyl cyanoacetate (11.5 ml, 108.53 mmol) were dissolved in anhydrous toluene (100 ml). Sodium acetate (4 g) and acetic acid (8 ml) were added. The reaction mixture was refluxed at 130 ° C for 48 hrs. Second lot of sodium acetate (2 g) and acetic acid (4 ml) were added after 12 hrs. Water generated in the reaction mixture was removed by using dean stark apparatus. On cooling water was added in the reaction mixture and extracted with ethyl acetate (100 ml x 3). The combined organic phases were concentrated under vacuum and purified by column chromatography using 5 % EtOAc in hexane as the eluent to get the pure product (8.9 g, 52.72 %). ^1H NMR (500 MHz, CDCl_3): δ 6.65 (m, 1H), 4.24-4.26 (q, 2H), 2.88

(s, 2H), 2.53 (s, 2H), 1.96 (s, 3H), 1.32-1.35 (t, 3H), 0.98 (s, 3H), 0.96 (s, 3H); ^{13}C NMR (125 MHz, CDCl_3): δ 165.96, 162.50, 156.58, 120.48, 116.27, 98.15, 61.35, 45.69, 45.28, 31.72, 27.92, 25.45, 14.13, ppm.

3. Results and discussion

3.1 Photophysical properties

Absorption and emission properties of all the four styryl derivatives **TMS**, **TTMS**, **TDS** and **TTS** were studied in solvents of different polarities. Table 1 shows absorption and emission λ_{max} , Stokes shift in cm^{-1} and molar extinction coefficient in $\text{mol}^{-1}\text{cm}^{-1}$ of all the four dyes in different solvents. Fig. 2 represents combined absorption and emission spectra for all the four dyes. The first absorption shoulder peak around 300 nm is due to the π - π^* transition of the dye and the second peak near 500 nm is due to the intramolecular charge transfer transition (ICT) between donor group and acceptor moiety. Slight red shifted absorption spectra are observed when the number of withdrawing isophorone carbethoxy groups increased on triphenylamine moiety. Also with the increasing number of withdrawing groups on triphenylamine group, remarkable change in the molar extinction coefficient is observed (Fig. 2). The styryl derivative with three supporting methoxy donating groups and three strong withdrawing isophorone carbethoxy groups (**TTS**) shows highest molar extinction coefficient, while the styryl derivative with three supporting methoxy donating group and only one withdrawing isophorone carbethoxy group (**TTMS**) show the lowest molar extinction coefficient.

The absorption maxima λ_{max} as well as molar extinction coefficient increases in the order of **TTMS** < **TMS** < **TDS** < **TTS** suggesting that as the number of isophorone carbethoxy groups increases from **TTMS** to **TTS** better intramolecular charge transfer (ICT) occurred from donor

triphenylamine to withdrawing isophorone carbethoxy groups. In the absorption spectra a shoulder peak around 375 nm for the isophorone moiety increases as the number of isophorone carbethoxy groups increases from **TTMS** to **TTS**. In the emission spectra same trend is observed i.e. emission intensity increases from **TTMS** to **TTS**, but very slight red shift in emission λ_{\max} is observed even after increasing the number of withdrawing isophorone carbethoxy groups. Similarly due to the additional methoxy groups in **TTMS** derivative as compared to the only one methoxy group in **TMS** derivative shows slightly red shifted absorption and emission λ_{\max} . So it can be predicted that there is a better intramolecular charge transfer (ICT) after varying the number of withdrawing groups instead the donating groups on triphenylamine.

Different photophysical parameters calculated from the available absorption and emission data are represented in Table 1 for all four dyes in chloroform solvent. Table 2 and S1-S3 represents the photophysical parameters calculated in set of non-polar to polar solvents for dyes **TTMS** and **TMS** to **TTS** respectively. It is observed that all four dyes exhibited slightly red shifted absorption spectra and highly red shifted emission spectra from non-polar to polar solvents. All four dyes show very high value of full width half maximum (FWHM) and hence they can be treated as very good energy absorbing dyes for their optoelectronic applications, further its value increases from non-polar to polar solvents. The value of oscillator strength (f) and transition dipole moment (μ_{eg}) were calculated from integrated absorption spectra using well-known expressions [67]. It is observed that as we go from mono to tri-styryl derivatives both the values increases and the highest value of oscillator strength (3.27) and transition dipole moment (18.80 Debye) were reported for the tri-styryl derivatives in DCM solvent. Similarly the values of radiative rate constant (Kr) in all solvents were calculated using Strickler Berg equation

$$Kr = 2.88 \times 10^{-9} n^2 \bar{\nu}_{av}^2 \int \epsilon_{\bar{\nu}} d\nu \quad (1)$$

Where $\bar{\nu}_{av}$ is the average wave number corresponding to the 0–0 transition and the integral part is evaluated from the area under the curve of absorption and emissions in all solvents. Again the highest Kr values were obtained for **TTS** dye. We also calculated the values of emission transition dipole moment, μ_{eg} (Ems) in all solvents by utilizing the value of Kr and integrated emission spectra [68] and it is found that these values are slightly lower than the transition dipole moment calculated from absorption spectra. No much variation in μ_{eg} (Ems) is observed when we go from non-polar to polar solvents.

<< **Please insert Fig. 2.** Combined Absorption and normalized emission spectra of dyes **TTMS**, **TMS**, **TDS** and **TTS** in chloroform solvent >>

<< **Please insert Fig. 3.** Absorption spectra of dye **TTMS** in all solvents>>

<< **Please insert Table 1.** Photophysical parameters of **TMS**, **TTMS**, **TDS** and **TTS** in chloroform solvent >>

<< **Please insert Table 2.** Photophysical properties of dye **TTMS** in all solvents >>

3.2 Solvatochromism, Lippert-Mataga correlation and Quantum yield of the dyes

The dyes were checked for their solvatochromism behavior in solvents of different polarity and red shifted emissions were observed after increasing the solvent polarity suggesting that the charge separation increases in the excited state which results in a larger dipole moment in the excited state as compared to the ground state. The absorption and emission spectra of dye **TTMS** in different polarity of solvents is shown in Fig.3 and Fig.4 respectively. A very good red shifted emission, 96 nm was observed for this dye from non-polar to polar solvent (Fig. 5). Similarly, remaining three dyes **TMS**, **TDS** and **TTS** also show red shifted emission of 95 nm, 88 nm and 93 nm respectively from non-polar to polar solvents (Fig.S2-S9). In polar solvents, emission intensity increases for dye **TTMS** and **TMS**, and decreases for dye **TDS** and **TTS**. Also for all

four dyes Stokes shift increases with the increase in the solvent polarity suggesting that these dyes have polar excited state and it is more stabilized in the polar solvent.

All the dyes emit in the red to deep-red region from 568 to 670 nm and also show red solid state fluorescence. The dyes **TDS** and **TTS** show the highest quantum yields in dioxane and the lowest one in acetonitrile solvent. The dye **TMS** show highest quantum yield in chloroform and lowest one in hexane solvent, while the dye **TTMS** shows the highest quantum yield in DMSO and the lowest one in hexane. In general the dyes **TDS** and **TTS** showed higher quantum efficiencies in non-polar solvents and lower quantum efficiencies in polar solvents, while the trend is opposite for **TTMS** and **TMS** dyes. This can be correlated with the observed quenching of fluorescence in polar solvents for **TDS** and **TTS** dyes and in non-polar solvents for **TTMS** and **TMS** dyes. As we predicted that dyes **TTMS** and **TMS** showed intramolecular charge transfer (ICT) while dyes **TDS** and **TTS** showed twisted intramolecular charge transfer (TICT), which was further supported by their viscosity sensitivity study. The twisted charge transfer state of dyes **TDS** and **TTS** is more stabilized by polar solvents as compared to the non-polar solvents to deliver red shifted emissions and quenching of fluorescence.

<< **Please insert Fig 4.** Emission spectra of dye **TTMS** in all solvent >>

<< **Please insert Fig 5.** Normalized emission spectra of dye **TTMS** in all solvents >>

Solvatochromism observed in these compounds and gradual increase in Stokes shift with increase in the solvent polarity can be correlated by using Lippert-Mataga equation [69]. Lippert-Mataga equation is showing direct correlation of physical parameters of solvent i.e. dielectric constant, refractive index and change in dipole moment of the compound upon excitation with Stokes shift. It is a very general equation for the effect of solvent on emission properties and does not account for specific solvent-fluorophore interactions, for e.g. through hydrogen

bonding, etc. The plot of Stokes shift Vs Lippert-Mataga function for all the four dyes exhibited linear relationship suggesting that solvent parameters such as dielectric constant and refractive index are collectively responsible for the red shift in emissions (Fig.6). The individual plot of Stokes shift Vs orientation polarizability i.e. Lippert-Mataga function (Δf) for all four dyes in different solvents is also represented in Fig. S10-S13. As Mac Rae is the improved version of Lippert-Mataga where in addition to the solvent polarizability, solute polarizability is also taken into account [70]. We found linear relationship between the plots of Mac Rae function (Δf_{MR}) Vs Stokes shift for all four derivatives in different solvent as shown in Fig. S14. This suggests that the polarity originated from the dipole created by the solute particles i.e. styryl dyes also contributed for the solvatochromic shift observed in polar solvents.

<< Please insert Fig. 6. Lippert-Mataga solvent polarity graphs for all four dyes >>

3.3 Multilinear regression analysis of absorption and emission shift using Kamlet-Taft and Catalan parameters

It is found that the single parameter scale such as Lippert-Mataga, Mac-Rae, and E_T^N (30) are inappropriate to explain exactly which solvent property or solute-solvent interaction is responsible for the observed solvent dependent physicochemical changes. Hence a multi-parameter approach proposed by Kamlet-Taft and Catalan is preferred and has been successfully applied to various physicochemical processes for e.g., UV-Visible absorption spectra, emission maxima in fluorescence spectra, Stokes shifts, quantum yield, radiative and non-radiative rate constants, fluorescence life time, etc.

In general the multi-linear expression is given as

$$y = y_0 + aA + bB + cC + dD \quad (2)$$

Where y is the solvent affected physiochemical property, y_0 is the studied physiochemical property in the gas phase. When all other solvent parameters are absent, then $y = y_0$. a , b , c and d are adjustable coefficients which reflect the dependence of y to the various {A, B, C, D} solvent parameters. We studied three different physiochemical properties (y) namely absorption maxima ($\bar{\nu}_{\text{abs}}$), emission maxima ($\bar{\nu}_{\text{emi}}$) and Stokes shift ($\Delta\bar{\nu}$). Among various solvent scales available in the literature, those provided by Kamlet and Taft [71,72] is most frequently used and is expressed as...

$$y = y_0 + a_{\alpha}\alpha + b_{\beta}\beta + c_{\pi^*}\pi^* \quad (\text{Kamlet-Taft}) \quad (3)$$

Where α represents effect of acidity (hydrogen-bond donating ability) of solvent, β represents effect of basicity (hydrogen-bond accepting ability) of solvent and π^* represents the collective effect of solvent polarity (also known as dipolarity) and polarizability. But if acidity or basicity of solvents is not affecting on the value of y , then among polarity and polarizability it is difficult to sort out which factor is exactly influencing the studied physiochemical property y , hence Catalan[73–75] proposed another expression...

$$y = y_0 + a_{\text{SA}}\text{SA} + b_{\text{SB}}\text{SB} + c_{\text{SP}}\text{SP} + d_{\text{SdP}}\text{SdP} \quad (\text{Catalan}) \quad (4)$$

Here total four solvent parameters namely SA (solvent acidity), SB (solvent basicity) SP (solvent polarizability) and SdP (solvent dipolarity) were introduced and the newly introduced parameter solvent dipolarity (SdP) can make difference between the exact contribution of solvent polarizability (SP) and solvent dipolarity (SdP). Also the individual solvatochromic parameters explained by Catalan are based on well-defined reference processes as opposed to the Kamlet-Taft parameters which are based on the average of several solvent-dependent processes.

To study our highly red shifted emission spectra and very high Stokes shift observed for all four styryl derivatives in polar solvents we used both, the well-established Kamlet-Taft as well as its improved version by Catalan simultaneously to understand exactly which factor i.e. solvent acidity, basicity, polarizability or dipolarity is mainly affecting the altered photophysical properties of these styryl derivatives in solvents of different polarities.

Multi-linear analysis of **TMS** is carried out in nine different solvents using absorption, emission and Stokes shift data. For the absorption data of this dye comparatively poor fit by both the methods is observed but Catalan parameter shows better correlation coefficient ($r = 0.65$) than Kamlet-Taft parameters ($r = 0.29$). Estimated coefficients for **TMS** dye by Kamlet-Taft and Catalan method are represented in Table 3. Large standard errors observed on both Kamlet-Taft and Catalan parameters for solvent acidity and basicity factors suggest that mainly solvent dipolarity or polarizability are responsible for the slightly red shifted absorption spectra. Also as a very high standard error is observed on solvent dipolarity (d_{SP}) factor, solvent polarizability (c_{SAP}) factor obtained by Catalan method can be considered as mainly responsible for the slightly red shifted absorption spectra. In the case of emission spectra again Catalan parameters show better correlation coefficient ($r = 0.98$) than Kamlet-Taft parameters (0.83). The negative value observed for all four solvent parameters (acidity, basicity, dipolarity and polarizability) both by Kamlet-Taft and Catalan analysis supports the red shifted emissions observed in polar solvents. Very small correlation coefficient observed for solvent acidity and basicity factors as well as very high standard error observed for the collective parameters of solvent polarizability as well as dipolarity, Kamlet-Taft method hasn't provide any conclusive result. Also for Catalan parameters very small correlation coefficient is observed for solvent acidity as well as basicity parameters when individually plotted with emission spectra, hence they cannot be considered for

the further analysis of emission spectra. Among solvent polarizability and dipolarity, though by first observation comparatively high standard error is observed for solvent dipolarity factor, it is also showing very high correlation coefficient (0.96) when individually plotted with the emission spectra. Hence solvent dipolarity (c_{SdP}) can be considered as the main factor responsible for the highly red shifted emission spectra of **TMS** dye. The graph plot of estimated emission values against experimental emission values shows excellent linear relation by Catalan parameters (slope = 0.99) (Fig. 7).

<< **Please insert Table 3.** Estimated coefficients (y_0 , a , b , c , d), their standard errors and correlation coefficients (r) for the multi-linear analysis of ($\bar{\nu}_{abs}$), ($\bar{\nu}_{emi}$) and ($\Delta\bar{\nu}$) of **TMS** as a function of Kamlet-Taft (2) and Catalan (3) solvent scales. Where, α or SA for solvent acidity, β or SB for solvent basicity, π^* for collective parameter of solvent dipolarity and polarizability according to Kamlet-Taft equation, SdP and SP for solvent dipolarity and polarizability respectively according to Catalan equation>>

As like **TMS** dye multilinear regression analysis using Kamlet-Taft and Catalan parameters is carried out for other three dyes i.e. **TDS**, **TTS** and **TTMS** and it is observed that for **TDS** and **TTS** dyes again Catalan parameters show better correlation coefficient than Kamlet-Taft parameters, but in the case of **TTMS** dye both the parameters are not showing very high correlation coefficient. Estimated coefficients for dyes **TDS**, **TTS** and **TTMS** by Kamlet-Taft and Catalan method are represented in Table S4. By seeing the sign of the each estimated coefficient as well as the extent of standard error and correlation coefficient obtained by both the methods, solvent dipolarity is emerged out as the main factor responsible for the shift in absorption as well as emission spectra, which was further supported by plotting absorption or emission data with each individual factor. Hence solvent dipolarity can be considered as the

main factor responsible for the slightly red shifted absorption as well as highly red shifted emission spectra of **TDS** and **TTS** dye. For red shifted emission spectra of **TTMS** dye again solvent dipolarity is the main factor responsible, but no any conclusive results were obtained to explain the slightly red shifted absorption spectra of this dye. The graph plot of estimated emission values against experimental emission values for dyes **TDS**, **TTS** and **TTMS** are represented by Fig. 7 which shows excellent linear relation with slope of 0.9776, 0.9765 and 0.7614 respectively.

<< **Please insert Fig. 7.** Correlation between experimental and predicted emission wave number for **TMS** (a), **TDS** (b), **TTS** (c) and **TTMS** (d) by Catalan method. >>

3.4 Intramolecular and twisted intramolecular charge transfer (ICT and TICT)

We studied the optical properties of all four dyes i.e. **TMS**, **TDS**, **TTS** and **TTMS** in different solvents. In general in the case of donor-acceptor compounds the polarity of solvents strongly affects the excited state of the molecule by stabilizing it through dipole-dipole, hydrogen bonding, and solvation interactions. In the excited state, such type of compounds instead of emitting from locally excited (LE) or Franck-Condon state they emit through newly generated intramolecular charge transfer (ICT) state or twisted intramolecular charge transfer state (TICT) state which is well-stabilized by polar solvents. In our case, emission spectra of all four dyes show very good positive solvatochromism from non-polar to polar solvents and all the emission peaks are very broad suggesting that they are not emitting through locally excited (LE) state but through ICT or TICT state. There are number of reports in the literature explaining the ICT and TICT emission. After seeing emission spectra of all four dyes, interestingly we found that **TMS** and **TTMS** dyes show enhancement of fluorescence in polar solvents while **TDS** and **TTS** dyes show quenching of fluorescence in polar solvents (Fig. 8). As all four dyes consisting of same

donor i.e. triphenylamine and same acceptor i.e. isophorone unit, the only difference is the number of donating or withdrawing groups. Recently it is proved that the free rotations of phenyl rings around single bond non-radiatively deactivates the excited state to a large extent through the formation of TICT state and as the number of such freely rotating group increases the chances of formation of TICT state is also increases [76]. In the case of styryl dyes as the number of double bond increases, though there is red shift in emission but at the same time lowering of fluorescence quantum yield observed due to the increased flexible units. It is also proved that in the case of styryl dyes, the main non-radiative decay channel is not the rotation around C-C bond, but the rotations around the dicyanovinyl C=C bond in the excited state [59]. In our case **TMS** and **TTMS** dyes having only one withdrawing unit, hence possibly emitting through the ICT state where no any fluorescence quenching in polar solvents is observed. In the case of **TDS** and **TTS** dyes, two and three withdrawing isophorone units are present respectively and hence more number of double bonds are present which may forcing the dye to emit through the TICT state after excitation. It is observed that the compounds emitting through TICT state, get twisted in the excited state where donor and acceptor moieties are mutually perpendicular to each other and total charge separation between the donor and acceptor is observed, which further elevates the HOMO level to narrow the band gap. This TICT state is stabilized by polar solvents to give bathochromically shifted emission, but at the same time it is susceptible for the various non-radiative quenching processes and shows quenching of fluorescence in polar solvents. The TICT emissions can be blocked chemically by restricting the rotations around single bond by designing structure of compounds having bulkier groups in vicinity.

Now-a-days instead of taking lot of synthetic efforts to make such type of rigid structures researchers tried to enhance the fluorescence of such TICT fluorophores through AIE effect,

viscosity study or by studying the fluorescence at lower temperature. To support our above observations we also studied the viscosity effect on the fluorescence properties of all four styryl dyes and found better fluorescence enhancement for dyes **TDS** and **TTS** as compared to dyes **TMS** and **TTMS**.

<< **Please insert Fig. 8.** Emission spectra of compound **TMS**, **TTMS**, **TDS** and **TTS** in all solvents. Designed line represents non-polar solvents while plane line represents polar solvents
>>

3.5 Viscosity sensitivity and twisted intramolecular charge transfer (TICT)

To correlate our above experimental findings i.e. quenching or enhancement of fluorescence from non-polar to polar solvents we studied the viscosity sensitivity of these styryl dyes in ethanol: PEG 400 mixture of solvents. Due to its extra phenyl rings rotating around single bond the triphenylamine based styryl dyes already reported to show enhanced fluorescence after hindering the rotation in viscous media [59]. In the case of styryl dyes **TDS** and **TTS**, quenching of fluorescence is observed as polarity of solvent increases and we proposed that these emissions are due to the TICT state formed in polar solvents. Hence instead of using polar solvent like glycerol for viscosity study we used polyethylene glycol 400, which is comparatively non-polar and less toxic commercially used viscous solvent. In 5 μM solutions of these dyes in ethanol percentage of PEG increased from 10 to 100 % where enhancement of fluorescence was observed with the increased percentage of PEG. Fig. 9 represents viscosity induced emission of all four styryl dyes with increasing percentage of PEG 400 in ethanol. We found 2.24 and 2.64 times enhancement of fluorescence for **TMS** and **TTMS** dye respectively, which is almost doubled for **TDS** and **TTS** dye and they show 4.03 and 5.02 times fluorescence enhancement respectively. As we proposed earlier that the very high fluorescence enhancement observed for

TDS and **TTS** dye is due to the formation of TICT state in the excited state which get blocked in viscous media and show increased fluorescence with slightly blue shifted emission spectra. In between **TDS** and **TTS** comparatively better enhancement in fluorescence is observed for **TTS** dye which possessing highest number of withdrawing groups in all four dyes. Due to their good sensitivity to viscous media styryl dyes **TDS** and **TTS** can be considered as fluorescent molecular rotors (FMRs) as they show very higher emission wavelengths (637 and 641nm for **TDS** and **TTS** respectively) as compared to well-known traditional FMR 1 (2-(4-(dimethylamino)benzylidene)malononitrile, at 460 nm). Similarly they show very high Stokes shift (128 and 131 nm for **TDS** and **TTS** dyes respectively) as compared to 40 nm for FMR 1. Due to its biological importance viscosity sensitivity above 600 nm is highly essential and there are very few reports till date for the viscosity sensitivity in this region. As all our styryl dyes emits above 600 nm due to their methoxy they can be considered as a very good FMRs in the deep red region.

<< Please insert Fig. 9. Emission spectra of compound **TMS(I)**, **TDS(II)**, **TTS (III)** and **TTMS(IV)** in mixture of ethanol and PEG 400 >>

3.6 Electrochemical Properties

To study their redox behavior we performed cyclic voltametry study of these dyes in dichloromethane using tetrabutylammonium hexafluorophosphate (NBu_4PF_6) as electrolyte at a scan rate of 100 mV/s, where ferrocene is used as reference standard. The cyclic voltammograms are displayed in Fig. 10. The observed main oxidation peak for these styryl derivatives are mainly due to the removal of electron from central nitrogen atom of triphenylamine and the extra oxidation peaks observed for dyes **TMS**, **TDS** and **TTMS** are may be due to the removal of

electron from extra methoxy groups present on triphenylamine donor though they are not in direct conjugation with the withdrawing isophorone unit. First oxidation peak observed for all four dyes is at around 0.84 to 0.92 mV/s in which dyes **TMS** and **TTMS** shows lowest oxidation potential at 0.8410 mV/s and dye **TTS** shows highest oxidation potential at 0.9178 mV/s. Except dye **TTS**, remaining three dyes show second oxidation peak at around 1.50 mV/s confirming the supporting donating ability of extra methoxy groups present on main triphenylamine donor. Due to the two more extra methoxy groups present on **TTMS** dye, it shows one more oxidation peak at 1.1333 mV/s. Also due to its highly symmetric structure and unavailability of electron for removal due to the more number of withdrawing isophorone unit present on **TTS** dye it shows only one oxidation peak at 0.9178 mV/s.

<< **Fig.10** Cyclic voltammograms of dye **TMS**, **TDS**, **TTS** and **TTMS** in DCM at room temperature >>

3.7 Comparative photophysical properties of plain and methoxy supported triphenylamine-isophorone styryls:

Recently donor capability of triphenylamine is further improved by decorating the extra phenyl rings of triphenylamine with additional donating groups such as carbazole [19], phenothiazine [46], etc and such starburst triphenylamine based dyes are utilized for Dye-sensitized solar cell applications, but due to the steric hindrance they are not reported to show very high efficiency for dye sensitized solar cell, hence small donating groups such as methoxy are preferred over bulkier groups [48]. We have synthesized different triphenylamine styryl dyes with extra methoxy groups as supporting donor. Though these methoxy groups are not in direct conjugation with the withdrawing groups, they improved total donating ability of triphenylamine and show

red shifted absorptions as well as emissions than the plane triphenylamine styryl dyes reported recently [61]. We developed a novel synthetic strategy to get these methoxy triphenylamine intermediates 3, 4 and 5. Due to the presence of methoxy at ortho position, substitution at para position of the triphenylamine nitrogen was found easier and we synthesized the tri-formylated derivative of triphenylamine in a very good yield. We compared the photophysical properties such as absorption, emission and Stokes shift of these newly synthesized dyes with recently reported dyes by Zhou et al, where they used same donor-acceptor combination but on plane triphenylamine [61]. The comparative photophysical properties of mono-substituted (**Compound 1**), di-substituted (**Compound 3**) and tri-substituted (**Compound 5**) dyes with our methoxy supported dyes **TMS**, **TTMS**, **TDS** and **TTS** are shown in Table 4. We found red shifted absorption and emission values for the methoxy supported dyes. In the case of **TTMS** dye which is having two more methoxy groups than **TMS** dye also shows red shifted absorptions as well as emissions than **compound 1**(reported dye) as well as **TMS** dye which possessing only one extra methoxy group. But after putting extra methoxy groups, no much more variation in Stokes shift is observed. Fig. 11 represents the effect of additional methoxy groups on absorption and emission λ_{\max} of these styryl dyes.

<< **Please insert Fig.11:** Comparative photophysical properties of **Comp 1**(reported dye), **TMS** and **TTMS** dye >>

<< **Please insert Table 4.** Comparative photo-physical properties of the plain triphenylamine isophorone styryl (blue color) and methoxy supported triphenylamine based styryl (red color) dyes in different solvents >>

3.8 Optimized geometries of the styryl dyes

We optimized the molecular structure of these dyes in the gas phase using time-dependent density functional theory (TD-DFT) calculations with the Gaussian 09 program using the B3LYP functional [63,64,77]. Optimized molecular structures together with the frontier molecular orbital profiles displaying electronic distributions in their HOMO and LUMO in gas phase are displayed in Fig. 09. Minimum overlap of electron density between HOMO and LUMO is observed in the case of dyes **TMS** and **TTMS** as compared to the dyes **TDS** and **TTS** suggesting that more effective charge transfer is possible in the case of mono-styryls as compared to the di and tri-styryls. At HOMO level maximum electron density is located on the donating triphenylamine phenyl rings while at LUMO level it is shifted towards the withdrawing isophorone unit. In the case of **TTS** dye, though the whole electron density is located on the methoxy supported triphenylamine donor part at HOMO level, it is shifted towards only two withdrawing styryl unit at LUMO level and one of the withdrawing isophorone unit remained totally vacant, hence it is not at all taking part in the charge transfer mechanism. Table S5 to S8 represents the respective Cartesian coordinates for all four dyes. The energy gap between HOMO and LUMO for all four dyes were calculated at gas phase and are represented in Fig. 12, whereas expected **TTS** dye shows lowest difference between HOMO-LUMO energy (2.52 eV) due to the extended conjugation and highest number of withdrawing isophorone unit among all four derivatives and **TMS** dye shows highest difference between HOMO-LUMO energy (2.67 eV) due to the single withdrawing unit.

<< **Please insert Fig. 12.** HOMO-LUMO FMO diagrams of dye **TMS**, **TTMS**, **TDS** and **TTS** in gas phase at ground state >>

<< **Please insert Fig. 13.** HOMO-LUMO energy gaps of dyes **TMS**, **TDS**, **TTS** and **TTMS** in gas phase >>

The computationally derived lowest energy transitions i.e. vertical excitations, oscillator strengths and dipole moments in gas phase were compared with the experimentally observed absorptions, oscillator strength and dipole moment derived from absorption λ_{max} in hexane solvent [Table 5]. In general computationally observed vertical excitation values are well in agreement with the experimental one with percentage deviation from 6.22 to 11.78 %. Major contribution of electronic transitions for all four dyes is from HOMO to LUMO (97-99 %). Almost similar trend for the experimentally derived and computationally observed oscillator strength is found and only exception is of **TTS** dye which shows almost double value of experimental oscillator strength than that observed computationally. Though the experimentally calculated dipole moment increases when we go from mono to tri-styryl dyes opposite trend is observed for the computationally derived one.

<< **Please insert Table 5.** Comparative experimental and computational photophysical parameters of **TMS**, **TDS**, **TTS** and **TTMS** in gas phase (computational method) and hexane solvent (experimental method) >>

4. Conclusion

Novel synthetic strategy has been developed to acquire methoxy supported mono, bis and tris methoxy supported triphenylamine aldehyde as well as respective styryl dyes. Due to the supporting methoxy groups donating ability of triphenylamine was increased and all the newly synthesized styryl derivatives showed red-shifted absorptions as well as emissions as compared to the known styryl derivatives on plane triphenylamine. Additionally as the number of withdrawing isophorone unit increases on triphenylamine both molar extinction coefficient as well as emission intensity increases from mono to tri-substituted triphenylamine. Kamlet-Taft

and Catalan multilinear analysis of absorption and emission spectra has shown that mainly solvent dipolarity factor is responsible for the slightly red shifted absorption spectra as well as highly red shifted emission spectra. Three oxidation peaks observed for **TTMS** dye confirms the involvement of extra methoxy groups in the donor-acceptor skeleton. We segregated all four styryl derivatives into two groups as ICT (**TMS**, **TTMS**) and TICT (**TDS**, **TTS**) dyes depending on their moderate and very high viscosity sensitivity respectively.

Acknowledgements

Author SSK is thankful for University Grants Commission (UGC), India as well as Technical Education Quality Improvement Program (TEQIP) for a Research Fellowship. We are also thankful to the Sophisticated Analytical Instrument Facility (SAIF), IIT, Mumbai, India for the recording of mass and HR-MS spectra.

Appendix A. Supplementary data

Supplementary data related to this article can be found at.....

References

- [1] Wei P, Bi X, Wu Z, Xu Z. Synthesis of Triphenylamine-Cored Dendritic Two-Photon Absorbing Chromophores. *Org Lett* 2005;7:3199–202. doi:10.1021/ol050905n.
- [2] Hrobárik P, Hrobáriková V, Sigmundová I, Zahradník P, Fakis M, Polyzos I, et al. Benzothiazoles with Tunable Electron-Withdrawing Strength and Reverse Polarity: A Route to Triphenylamine-Based Chromophores with Enhanced Two-Photon Absorption. *J Org Chem* 2011;76:8726–36. doi:10.1021/jo201411t.
- [3] Porrès L, Mongin O, Katan C, Charlot M, Pons T, Mertz J, et al. Enhanced Two-Photon Absorption with Novel Octupolar Propeller-Shaped Fluorophores Derived from Triphenylamine. *Org Lett* 2004;6:47–50. doi:10.1021/ol036041s.

- [4] Lartia R, Allain C, Bordeau G, Schmidt F, Fiorini-Debuisschert C, Charra F, et al. Synthetic Strategies to Derivatizable Triphenylamines Displaying High Two-Photon Absorption. *J Org Chem* 2008;73:1732–44. doi:10.1021/jo702002y.
- [5] Xu B, Fang H, Chen F, Lu H, He J, Li Y, et al. Synthesis, characterization, two-photon absorption, and optical limiting properties of triphenylamine-based dendrimers. *New J Chem* 2009;33:2457–64. doi:10.1039/B9NJ00393B.
- [6] Zeng S, Ouyang X, Zeng H, Ji W, Ge Z. Synthesis, tunable two and three-photon absorption properties of triazine derivatives by branches. *Dye Pigment* 2012;94:290–5. doi:http://dx.doi.org/10.1016/j.dyepig.2012.01.014.
- [7] Zhang X, Ren X, Xu Q-H, Loh KP, Chen Z-K. One- and Two-Photon Turn-on Fluorescent Probe for Cysteine and Homocysteine with Large Emission Shift. *Org Lett* 2009;11:1257–60. doi:10.1021/ol802979n.
- [8] Wang X, Wang D, Zhou G, Yu W, Zhou Y, Fang Q, et al. Symmetric and asymmetric charge transfer process of two-photon absorbing chromophores: bis-donor substituted stilbenes, and substituted styrylquinolinium and styrylpyridinium derivatives. *J Mater Chem* 2001;11:1600–5. doi:10.1039/B009769L.
- [9] Lupton JM, Samuel IDW, Burn PL, Mukamel S. Control of intrachromophore excitonic coherence in electroluminescent conjugated dendrimers. *J Phys Chem B* 2002;106:7647–53. doi:10.1021/jp020418e.
- [10] Lee HJ, Sohn J, Hwang J, Park SY, Choi H, Cha M. Triphenylamine-Cored Bifunctional Organic Molecules for Two-Photon Absorption and Photorefractive. *Chem Mater* 2004;16:456–65. doi:10.1021/cm0343756.
- [11] Lee HJ, Sohn J, Hwang J, Park SY, Choi H, Cha M. Triphenylamine-Cored Bifunctional Organic Molecules for Two-Photon Absorption and Photorefractive. *Chem Mater* 2004;16:456–65. doi:10.1021/cm0343756.
- [12] Fang Z, Teo TL, Cai L, Lal YH, Samoc A, Samoc M. Bridged triphenylamine-based dendrimers: Tuning enhanced two-photon absorption performance with locked molecular planarity. *Org Lett* 2009;11:1–4. doi:10.1021/ol801238n.
- [13] Fang Z, Zhang X, Hing Lai Y, Liu B. Bridged triphenylamine based molecules with large two-photon absorption cross sections in organic and aqueous media. *Chem Commun (Camb)* 2009:920–2. doi:10.1039/b812649f.
- [14] Wu G, Kong F, Zhang Y, Zhang X, Li J, Chen W, et al. Multiple-Anchoring Triphenylamine Dyes for Dye-Sensitized Solar Cell Application. *J Phys Chem C* 2014;118:8756–65. doi:10.1021/jp4124265.

- [15] Qin P, Zhu H, Edvinsson T, Boschloo G, Hagfeldt A, Sun L. Design of an Organic Chromophore for P-Type Dye-Sensitized Solar Cells. *J Am Chem Soc* 2008;130:8570–1. doi:10.1021/ja8001474.
- [16] Haid S, Marszalek M, Mishra A, Wielopolski M, Teuscher J, Moser J-E, et al. Significant Improvement of Dye-Sensitized Solar Cell Performance by Small Structural Modification in π -Conjugated Donor–Acceptor Dyes. *Adv Funct Mater* 2012;22:1291–302. doi:10.1002/adfm.201102519.
- [17] Sakong C, Kim HJ, Kim SH, Namgoong JW, Park JH, Ryu J-H, et al. Synthesis and applications of new triphenylamine dyes with donor-donor-(bridge)-acceptor structure for organic dye-sensitized solar cells. *New J Chem* 2012;36:2025–32. doi:10.1039/C2NJ40374A.
- [18] Jia J, Zhang Y, Xue P, Zhang P, Zhao X, Liu B, et al. Synthesis of dendritic triphenylamine derivatives for dye-sensitized solar cells. *Dye Pigment* 2013;96:407–13. doi:http://dx.doi.org/10.1016/j.dyepig.2012.09.015.
- [19] Ning Z, Zhang Q, Wu W, Pei H, Liu B, Tian H. Starburst Triarylamine Based Dyes for Efficient Dye-Sensitized Solar Cells. *J Org Chem* 2008;73:3791–7. doi:10.1021/jo800159t.
- [20] Yao Y-S, Xiao J, Wang X-S, Deng Z-B, Zhang B-W. Starburst DCM-Type Red-Light-Emitting Materials for Electroluminescence Applications. *Adv Funct Mater* 2006;16:709–18. doi:10.1002/adfm.200500558.
- [21] Li J, Ma C, Tang J, Lee C-S, Lee S. Novel Starburst Molecule as a Hole Injecting and Transporting Material for Organic Light-Emitting Devices. *Chem Mater* 2005;17:615–9. doi:10.1021/cm048337d.
- [22] Zhang Q, Ning Z, Tian H. “Click” synthesis of starburst triphenylamine as potential emitting material. *Dye Pigment* 2009;81:80–4. doi:http://dx.doi.org/10.1016/j.dyepig.2008.09.005.
- [23] Liu Q-D, Lu J, Ding J, Day M, Tao Y, Barrios P, et al. Monodisperse Starburst Oligofluorene-Functionalized 4,4',4''-Tris(carbazol-9-yl)-triphenylamines: Their Synthesis and Deep-Blue Fluorescent Properties for Organic Light-Emitting Diode Applications. *Adv Funct Mater* 2007;17:1028–36. doi:10.1002/adfm.200600104.
- [24] Pan B, Huang H, Yang X, Jin J, Zhuang S, Mu G, et al. Systematic study of TCTA-based star-shaped host materials by optimizing ratio of carbazole/ diphenylphosphine oxide: achieving both low efficiency roll-off and turn-on voltage for blue PHOLEDs. *J Mater Chem C* 2014;2:7428–35. doi:10.1039/C4TC00951G.
- [25] Kochapradist P, Prachumrak N, Tarsang R, Keawin T, Jungsuttiwong S, Sudyoadsuk T, et al. Multi-triphenylamine-substituted carbazoles: synthesis, characterization, properties,

- and applications as hole-transporting materials. *Tetrahedron Lett* 2013;54:3683–7. doi:<http://dx.doi.org/10.1016/j.tetlet.2013.05.007>.
- [26] Zhou G, Wong W-Y, Yao B, Xie Z, Wang L. Triphenylamine-Dendronized Pure Red Iridium Phosphors with Superior OLED Efficiency/Color Purity Trade-Offs. *Angew Chemie Int Ed* 2007;46:1149–51. doi:10.1002/anie.200604094.
- [27] Khanasa T, Prachumrak N, Rattanawan R, Jungsuttiwong S, Keawin T, Sudyoadsuk T, et al. Bis(carbazol-9-ylphenyl)aniline End-Capped Oligoarylenes as Solution-Processed Nondoped Emitters for Full-Emission Color Tuning Organic Light-Emitting Diodes. *J Org Chem* 2013;78:6702–13. doi:10.1021/jo4008332.
- [28] Tang X, Liu W, Wu J, Lee C-S, You J, Wang P. Synthesis, Crystal Structures, and Photophysical Properties of Triphenylamine-Based Multicyano Derivatives. *J Org Chem* 2010;75:7273–8. doi:10.1021/jo101456v.
- [29] Misra R, Maragani R, Gautam P, Mobin SM. Tetracyanoethylene substituted triphenylamine analogues. *Tetrahedron Lett* 2014;55:7102–5. doi:<http://dx.doi.org/10.1016/j.tetlet.2014.10.148>.
- [30] Li Y, Ren T, Dong W-J. Tuning photophysical properties of triphenylamine and aromatic cyano conjugate-based wavelength-shifting compounds by manipulating intramolecular charge transfer strength. *J Photochem Photobiol A Chem* 2013;251:1–9. doi:<http://dx.doi.org/10.1016/j.jphotochem.2012.10.002>.
- [31] Pålsson L-O, Wang C, Batsanov AS, King SM, Beeby A, Monkman AP, et al. Efficient Intramolecular Charge Transfer in Oligoene-Linked Donor- π -Acceptor Molecules. *Chem – A Eur J* 2010;16:1470–9. doi:10.1002/chem.200902099.
- [32] Leriche P, Frère P, Cravino A, Alévêque O, Roncali J. Molecular Engineering of the Internal Charge Transfer in Thiophene-Triphenylamine Hybrid π -Conjugated Systems. *J Org Chem* 2007;72:8332–6. doi:10.1021/jo701390y.
- [33] Ishow E, Clavier G, Miomandre F, Rebarz M, Buntinx G, Poizat O. Comprehensive investigation of the excited-state dynamics of push-pull triphenylamine dyes as models for photonic applications. *Phys Chem Chem Phys* 2013;15:13922–39. doi:10.1039/C3CP51480C.
- [34] Pina J, Seixas de Melo JS, Batista RMF, Costa SPG, Raposo MMM. Triphenylamine-Benzimidazole Derivatives: Synthesis, Excited-State Characterization, and DFT Studies. *J Org Chem* 2013;78:11389–95. doi:10.1021/jo401803u.
- [35] Yuan WZ, Gong Y, Chen S, Shen XY, Lam JWY, Lu P, et al. Efficient Solid Emitters with Aggregation-Induced Emission and Intramolecular Charge Transfer Characteristics: Molecular Design, Synthesis, Photophysical Behaviors, and OLED Application. *Chem Mater* 2012;24:1518–28. doi:10.1021/cm300416y.

- [36] Li H, Chi Z, Xu B, Zhang X, Li X, Liu S, et al. Aggregation-induced emission enhancement compounds containing triphenylamine-anthrylenevinylene and tetraphenylethene moieties. *J Mater Chem* 2011;21:3760–7. doi:10.1039/C0JM02571B.
- [37] Liu Y, Chen S, Lam JWY, Lu P, Kwok RTK, Mahtab F, et al. Tuning the Electronic Nature of Aggregation-Induced Emission Luminogens with Enhanced Hole-Transporting Property. *Chem Mater* 2011;23:2536–44. doi:10.1021/cm2003269.
- [38] Wang B, Qian Y. Synthesis and efficient solid-state emission of conjugated donor-acceptor-donor triphenylamine chromophores. *New J Chem* 2013;37:1402–7. doi:10.1039/C3NJ41115J.
- [39] Yang M, Xu D, Xi W, Wang L, Zheng J, Huang J, et al. Aggregation-Induced Fluorescence Behavior of Triphenylamine-Based Schiff Bases: The Combined Effect of Multiple Forces. *J Org Chem* 2013;78:10344–59. doi:10.1021/jo401719c.
- [40] Zhao X, Xue P, Wang K, Chen P, Zhang P, Lu R. Aggregation-induced emission of triphenylamine substituted cyanostyrene derivatives. *New J Chem* 2014;38:1045–51. doi:10.1039/C3NJ01343J.
- [41] Ning Z, Chen Z, Zhang Q, Yan Y, Qian S, Cao Y, et al. Aggregation-induced Emission (AIE)-active Starburst Triarylamine Fluorophores as Potential Non-doped Red Emitters for Organic Light-emitting Diodes and Cl₂ Gas Chemodosimeter. *Adv Funct Mater* 2007;17:3799–807. doi:10.1002/adfm.200700649.
- [42] Zheng Z, Yu Z, Yang M, Jin F, Zhang Q, Zhou H, et al. Substituent Group Variations Directing the Molecular Packing, Electronic Structure, and Aggregation-Induced Emission Property of Isophorone Derivatives. *J Org Chem* 2013;78:3222–34. doi:10.1021/jo400116j.
- [43] Wang L, Shen Y, Zhu Q, Xu W, Yang M, Zhou H, et al. Systematic Study and Imaging Application of Aggregation-Induced Emission of Ester-Isophorone Derivatives. *J Phys Chem C* 2014;118:8531–40. doi:10.1021/jp412279m.
- [44] Li G, Zhou Y-F, Cao X-B, Bao P, Jiang K-J, Lin Y, et al. Novel TPD-based organic D-[small pi]-A dyes for dye-sensitized solar cells. *Chem Commun* 2009:2201–3. doi:10.1039/B822190A.
- [45] Tarsang R, Promarak V, Sudyoasuk T, Namuangruk S, Jungsuttiwong S. Tuning the electron donating ability in the triphenylamine-based D- π -A architecture for highly efficient dye-sensitized solar cells. *J Photochem Photobiol A Chem* 2014;273:8–16. doi:http://dx.doi.org/10.1016/j.jphotochem.2013.09.002.
- [46] Wan Z, Jia C, Duan Y, Zhou L, Lin Y, Shi Y. Phenothiazine-triphenylamine based organic dyes containing various conjugated linkers for efficient dye-sensitized solar cells. *J Mater Chem* 2012;22:25140–7. doi:10.1039/C2JM34682F.

- [47] Wan Z, Jia C, Duan Y, Zhou L, Zhang J, Lin Y, et al. Influence of the antennas in starburst triphenylamine-based organic dye-sensitized solar cells: phenothiazine versus carbazole. *RSC Adv* 2012;2:4507–14. doi:10.1039/C2RA01326F.
- [48] Kim SH, Choi J, Sakong C, Namgoong JW, Lee W, Kim DH, et al. The effect of the number, position, and shape of methoxy groups in triphenylamine donors on the performance of dye-sensitized solar cells. *Dye Pigment* 2015;113:390–401. doi:http://dx.doi.org/10.1016/j.dyepig.2014.09.014.
- [49] Im H, Kim S, Park C, Jang S-H, Kim C-J, Kim K, et al. High performance organic photosensitizers for dye-sensitized solar cells. *Chem Commun* 2010;46:1335–7. doi:10.1039/B917065K.
- [50] Tan L-L, Huang J-F, Shen Y, Xiao L-M, Liu J-M, Kuang D-B, et al. Highly efficient and stable organic sensitizers with duplex starburst triphenylamine and carbazole donors for liquid and quasi-solid-state dye-sensitized solar cells. *J Mater Chem A* 2014;2:8988–94. doi:10.1039/C4TA01351D.
- [51] Fang Z, Chellappan V, Webster RD, Ke L, Zhang T, Liu B, et al. Bridged-triarylamine starburst oligomers as hole transporting materials for electroluminescent devices. *J Mater Chem* 2012;22:15397–404. doi:10.1039/C2JM32840B.
- [52] Yen H-J, Lin H-Y, Liou G-S. Novel Starburst Triarylamine-Containing Electroactive Aramids with Highly Stable Electrochromism in Near-Infrared and Visible Light Regions. *Chem Mater* 2011;23:1874–82. doi:10.1021/cm103552k.
- [53] Haidekker M a, Theodorakis E a. Molecular rotors--fluorescent biosensors for viscosity and flow. *Org Biomol Chem* 2007;5:1669–78. doi:10.1039/b618415d.
- [54] Lakowicz JR, Masters BR. Principles of Fluorescence Spectroscopy, Third Edition. *J Biomed Opt* 2008;13:029901. doi:10.1117/1.2904580.
- [55] Jacobson a., Petric a., Hogenkamp D, Sinur a., Barrio JR. 1,1-Dicyano-2-[6-(dimethylamino)naphthalen-2-yl]propene (DDNP): A solvent polarity and viscosity sensitive fluorophore for fluorescence microscopy. *J Am Chem Soc* 1996;118:5572–9. doi:10.1021/ja9543356.
- [56] Grabowski ZR, Rotkiewicz K, Rettig W. Structural Changes Accompanying Intramolecular Electron Transfer: Focus on Twisted Intramolecular Charge-Transfer States and Structures. *Chem Rev* 2003;103:3899–4032. doi:10.1021/cr940745l.
- [57] Haidekker M a, Theodorakis E a. Environment-sensitive behavior of fluorescent molecular rotors. *J Biol Eng* 2010;4:11. doi:10.1186/1754-1611-4-11.

- [58] Yoon H-J, Dakanali M, Lichlyter D, Chang WM, Nguyen KA, Nipper ME, et al. Synthesis and evaluation of self-calibrating ratiometric viscosity sensors. *Org Biomol Chem* 2011;9:3530–40. doi:10.1039/C0OB01042A.
- [59] Zhou F, Shao J, Yang Y, Zhao J, Guo H, Li X, et al. Molecular Rotors as Fluorescent Viscosity Sensors: Molecular Design, Polarity Sensitivity, Dipole Moments Changes, Screening Solvents, and Deactivation Channel of the Excited States. *European J Org Chem* 2011;2011:4773–87. doi:10.1002/ejoc.201100606.
- [60] Gupta VD, Tathe AB, Padalkar VS, Umape PG, Sekar N. Red emitting solid state fluorescent triphenylamine dyes: Synthesis, photo-physical property and DFT study. *Dye Pigment* 2013;97:429–39. doi:http://dx.doi.org/10.1016/j.dyepig.2012.12.024.
- [61] Gan X, Wang Y, Ge X, Li W, Zhang X, Zhu W, et al. Triphenylamine isophorone derivatives with two photon absorption: Photo-physical property, DFT study and bio-imaging. *Dye Pigment* 2015;120:65–73. doi:http://dx.doi.org/10.1016/j.dyepig.2015.04.007.
- [62] Kohn W, Sham LJ. Self-Consistent Equations Including Exchange and Correlation Effects. *Phys Rev* 1965;140:A1133–8. doi:10.1103/PhysRev.140.A1133.
- [63] Becke AD. A new mixing of Hartree–Fock and local density-functional theories. *J Chem Phys* 1993;98:1372. doi:10.1063/1.464304.
- [64] Lee C, Yang W, Parr RG. Development of the Colle-Salvetti correlation-energy formula into a functional of the electron density. *Phys Rev B* 1988;37:785–9. doi:10.1103/PhysRevB.37.785.
- [65] Scalmani G, Frisch MJ, Mennucci B, Tomasi J, Cammi R, Barone V. Geometries and properties of excited states in the gas phase and in solution: theory and application of a time-dependent density functional theory polarizable continuum model. *J Chem Phys* 2006;124:94107. doi:10.1063/1.2173258.
- [66] Park KH, Twieg RJ, Ravikiran R, Rhodes LF, Shick RA, Yankelevich D, et al. Synthesis and Nonlinear-Optical Properties of Vinyl-Addition Poly(norbornene)s. *Macromolecules* 2004;37:5163–78. doi:10.1021/ma040044i.
- [67] Satam MA, Telore RD, Sekar N. Pigment Yellow 101 analogs from 3-(1,3-benzothiazol-2-yl)-2-hydroxynaphthalene-1-carbaldehyde – Synthesis and characterization. *Dye Pigment* 2015;123:274–84. doi:http://dx.doi.org/10.1016/j.dyepig.2015.08.015.
- [68] Lewis JE, Maroncelli M. On the (uninteresting) dependence of the absorption and emission transition moments of coumarin 153 on solvent. *Chem Phys Lett* 1998;282:197–203. doi:http://dx.doi.org/10.1016/S0009-2614(97)01270-0.

- [69] Lippert E. Spektroskopische Bestimmung des Dipolmomentes aromatischer Verbindungen im ersten angeregten Singulettzustand. *Zeitschrift Für Elektrochemie, Berichte Der Bunsengesellschaft Für Phys Chemie* 1957;61:962–75. doi:10.1002/bbpc.19570610819.
- [70] McRae EG. Theory of Solvent Effects on Molecular Electronic Spectra. Frequency Shifts. *J Phys Chem* 1954;61:1957. doi:10.1021/j150551a012.
- [71] Kamlet MJ, Taft RW. The solvatochromic comparison method. I. The .beta.-scale of solvent hydrogen-bond acceptor (HBA) basicities. *J Am Chem Soc* 1976;98:377–83. doi:10.1021/ja00418a009.
- [72] Kamlet MJ, Abboud JL, Taft RW. The solvatochromic comparison method. 6. The .pi.* scale of solvent polarities. *J Am Chem Soc* 1977;99:6027–38. doi:10.1021/ja00460a031.
- [73] Catalán J, López V, Pérez P, Martín-Villamil R, Rodríguez J-G. Progress towards a generalized solvent polarity scale: The solvatochromism of 2-(dimethylamino)-7-nitrofluorene and its homomorph 2-fluoro-7-nitrofluorene. *Liebigs Ann* 1995;1995:241–52. doi:10.1002/jlac.199519950234.
- [74] Catalán J, Díaz C. Extending the Solvent Acidity Scale to Highly Acidic Organic Solvents: The Unique Photophysical Behaviour of 3,6-Diethyltetrazine. *European J Org Chem* 1999;1999:885–91. doi:10.1002/(SICI)1099-0690(199904)1999:4<885::AID-EJOC885>3.0.CO;2-W.
- [75] Catalán J, Hopf H. Empirical Treatment of the Inductive and Dispersive Components of Solute–Solvent Interactions: The Solvent Polarizability (SP) Scale. *European J Org Chem* 2004;2004:4694–702. doi:10.1002/ejoc.200400311.
- [76] Hu R, Lager E, Aguilar-Aguilar A, Liu J, Lam JWY, Sung HHY, et al. Twisted Intramolecular Charge Transfer and Aggregation-Induced Emission of BODIPY Derivatives. *J Phys Chem C* 2009;113:15845–53. doi:10.1021/jp902962h.
- [77] Gaussian 09 Citation n.d. http://www.gaussian.com/g_tech/g_ur/m_citation.htm (accessed December 18, 2015).

Tables

Table 1. Photophysical parameters of TMS, TTMS, TDS and TTS in chloroform solvent

Solvent	λ_{abs}	$\epsilon_{\text{max}} \times 10^4$	fwhm	λ_{ems}	Stokes shift	Φ_{F}	f	$\mu_{\text{eg}}(\text{Abs})$	$\mu_{\text{eg}}(\text{Ems})$	Kr x (10^8)	
	(nm)	($\text{M}^{-1} \text{cm}^{-1}$)	(nm)	(nm)	(nm)	(cm^{-1})		(debye)	(debye)	(s^{-1})	
TMS	480	4.93	103	630	150	4960	0.025	1.04	10.33	9.18	3.05
TTMS	478	3.96	109	643	165	5368	0.029	0.81	9.07	7.50	2.02
TDS	509	8.04	127	637	128	3948	0.034	1.86	14.2	11.53	4.56
TTS	510	14.05	110	641	131	4007	0.043	2.73	17.22	14.14	6.63

Table 2. Photophysical properties of TTMS in all solvents

Solvent	λ_{abs}	$\epsilon_{\text{max}} \times 10^4$	fwhm	λ_{ems}	Stokes shift	Φ_{F}	f	$\mu_{\text{eg}}(\text{Abs})$	$\mu_{\text{eg}}(\text{Ems})$	Kr x (10^8)	
	(nm)	($\text{M}^{-1} \text{cm}^{-1}$)	(nm)	(nm)	(nm)	(cm^{-1})		(debye)	(debye)	(s^{-1})	
Hexane	467	5.00	90	572	105	3931	0.006	0.93	9.59	8.12	2.63
Toluene	475	4.29	97	594	119	4218	0.011	0.84	9.23	7.47	2.62
Dioxane	482	3.75	107	633	151	4949	0.028	0.84	9.27	7.38	2.09
Chloroform	478	3.96	109	643	165	5368	0.029	0.81	9.07	7.50	2.02
DCM	469	3.57	108	646	177	5842	0.017	0.77	8.75	7.33	1.75
Acetone	470	3.84	102	607	137	4802	0.012	0.79	8.87	7.82	1.7
EtOH	480	4.09	112	655	175	5566	0.021	0.9	9.61	8.17	1.81
Acetonitrile	468	3.66	111	659	191	6193	0.015	0.8	8.94	7.67	1.49
DMSO	483	3.45	116	667	184	5711	0.03	0.78	8.94	7.29	1.73

Table 3. Estimated coefficients (y_0 , a, b, c, d), their standard errors and correlation coefficients (r) for the multi-linear analysis of ($\bar{\nu}_{\text{abs}}$), ($\bar{\nu}_{\text{emi}}$) and ($\Delta\bar{\nu}$) of TMS as a function of Kamlet-Taft (2) and Catalan (3) solvent scales. Where, α or SA for solvent acidity, β or SB for solvent basicity, π^* for collective parameter of solvent dipolarity and polarizability according to Kamlet-Taft equation, SdP and SP for solvent dipolarity and polarizability respectively according to Catalan equation

Kamlet-Taft	$y_0 \times 10^3$	a_{α}	b_{β}	c_{π^*}	r
$\bar{\nu}_{\text{abs}}$	21.51 ± 0.23	-0.58 ± 0.43	0.55 ± 0.50	-0.98 ± 0.43	0.29
$\bar{\nu}_{\text{emi}}$	17.66 ± 0.30	-1.27 ± 0.56	-0.15 ± 0.65	-2.42 ± 0.56	0.83

$\Delta\bar{u}$	3.84 ± 0.43	0.69 ± 0.80	0.69 ± 0.93	1.44 ± 0.80		0.51
Catalan	$\gamma_0 \times 10^3$	a_{SA}	b_{SB}	c_{SDP}	d_{SP}	r
\bar{u}_{abs}	23.39 ± 0.65	-1.60 ± 0.68	0.49 ± 0.40	-0.38 ± 0.24	-3.06 ± 0.92	0.65
\bar{u}_{emi}	18.01 ± 0.40	-1.18 ± 0.42	0.06 ± 0.25	-2.28 ± 0.15	-0.79 ± 0.56	0.98
$\Delta\bar{u}$	5.38 ± 0.84	-0.42 ± 0.87	0.42 ± 0.51	1.89 ± 0.30	-2.26 ± 1.17	0.89

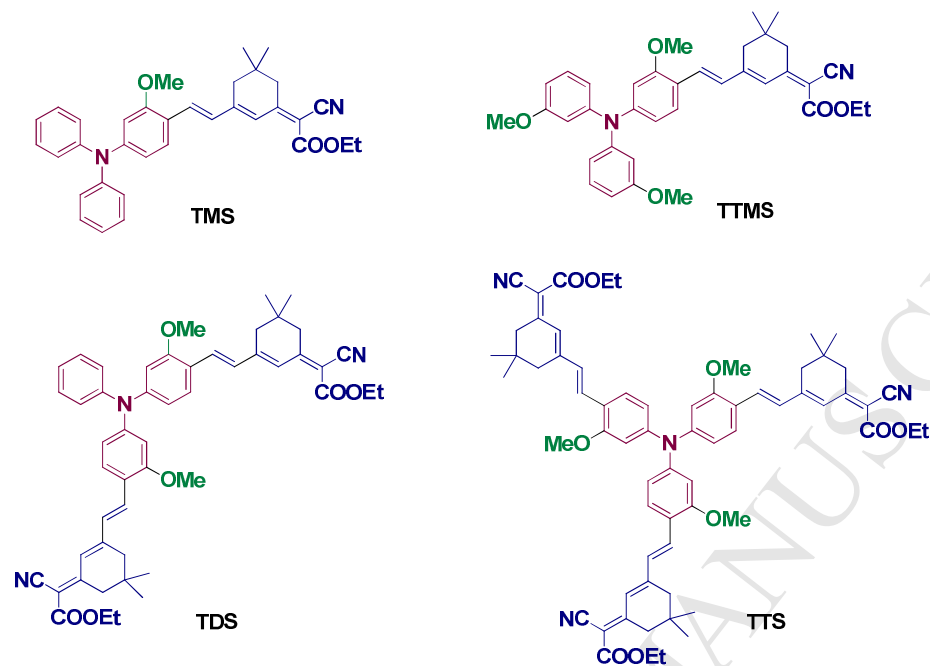
Table 4. Comparative photo-physical properties of the plain triphenylamine isophorone styryl (blue color) and methoxy supported triphenylamine based styryl (red color) dyes in different solvents.

Solvents	Comp 1 / TMS/TTMS			Comp 3 / TDS			Comp 5 / TTS		
	λ_{abs} (nm)	λ_{ems} (nm)	Stokes shift (cm^{-1})	λ_{abs} (nm)	λ_{ems} (nm)	Stokes shift (cm^{-1})	λ_{abs} (nm)	λ_{ems} (nm)	Stokes shift (cm^{-1})
Hexane	439/466/467	525/568/572	3731/3853/3931	482/489	538/574	2181/3028	482/492	547/584	2486/3202
Dioxane	438/469/482	570/603/633	5313/4738/4949	484/492	591/605	3740/3796	484/499	596/609	3882/3620
Chloroform	443/480/478	590/630/643	5649/4960/5368	498/509	615/637	3840/3948	496/510	618/641	4000/4007
EtOH	438/480/480	612/654/655	6517/5543/5566	493/507	614/644	4017/4196	482/507	611/655	4380/4457
Acetonitrile	429/469/468	617/657/659	7102/6101/6193	478/496	625/655	4942/4894	484/500	626/668	4686/5030

Table 5. Comparative experimental and computational photophysical parameters of TMS, TTMS, TDS and TTS in gas phase (computational method) and hexane solvent (experimental method)

Compound	λ_{abs}^a (nm)	λ_{abs}^b (nm)	λ_{ems}^c (nm)	f^d	f^e	μ_{eg}^f (debye)	μ_{eg}^g (debye)	% D^h	Major ⁱ Contribution	Total energy (eV)
TMS	466	495	568	1.12	1.2559	10.52	10.64	6.22	H → L 97.76	-44931.2
TTMS	467	496	572	0.93	1.2489	9.59	14.83	6.21	H → L 97.57	-69464.1
TDS	489	539	574	1.89	1.3936	14.03	12.10	10.22	H → L 97.49	-93997.1
TTS	492	550	531	2.44	1.1435	16.00	7.90	11.78	H → L 99.22	-51164

^aExperimental absorption λ_{max} , ^bComputational vertical excitation, ^cExperimental emission λ_{max} , ^dExperimentally calculated oscillator strength, ^eComputational oscillator strength, ^fExperimentally calculated transition dipole moment, ^gComputational dipole moment, ^hPercent deviation from experimental absorption λ_{max} , ⁱMajor electronic transition.

Figures**Fig. 1.** Structures of the synthesized dyes **TMS**, **TTMS**, **TDS** and **TTS**

Scheme 1. Synthesis of **TMS**, **TDS**, **TTS** and **TTMS** (a) Iodobenzene, potassium-t-butoxide, 1,10 Phenanthroline / CuI, toluene (b) 3-bromo anisole, potassium-t-butoxide, 1,10 Phen / CuI, toluene (c) DMF/POCl₃ (d) DMF/POCl₃, 1,2 dichloroethane (e) 11, piperidine, ethanol (f) ethyl cyanoacetate, NH₄OAc, acetic acid, toluene.

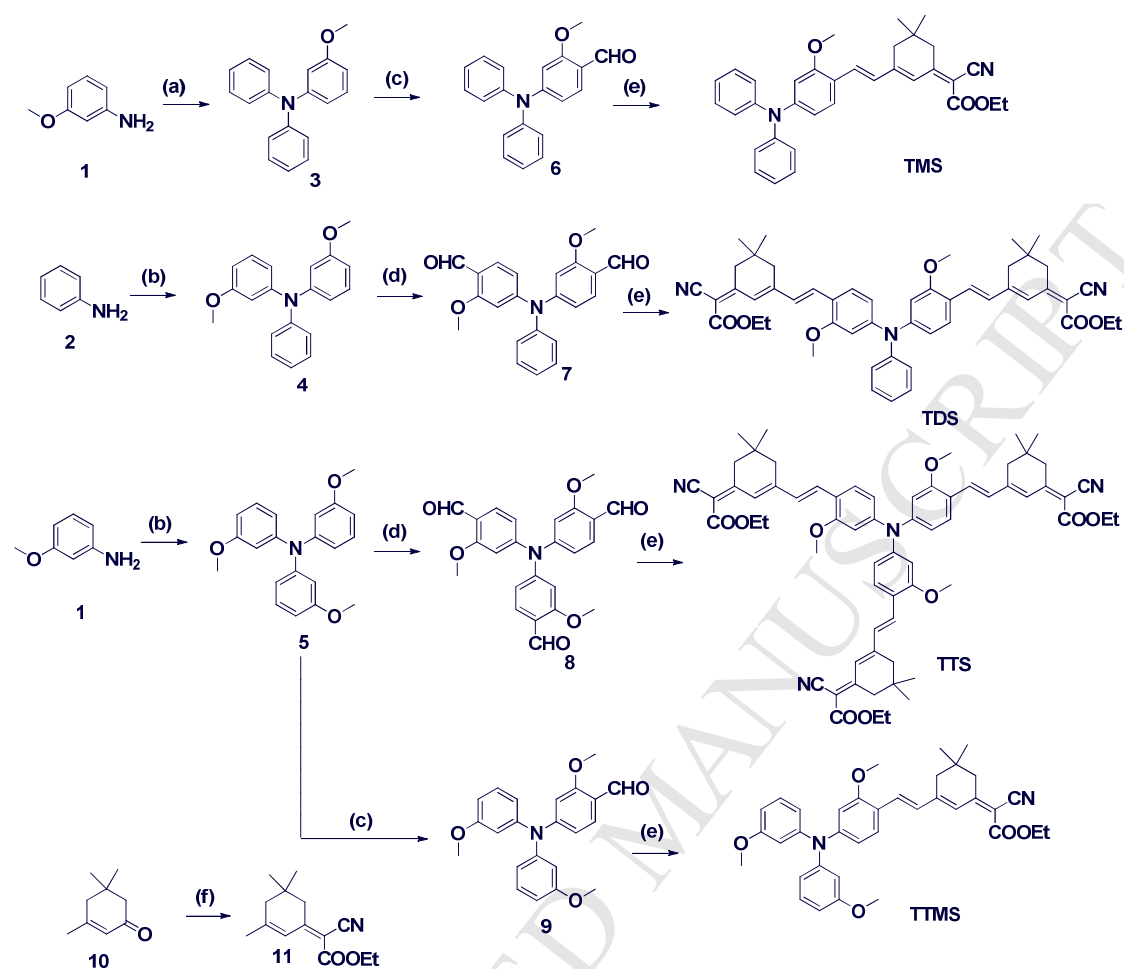


Fig. 2. Combined Absorption and normalized emission spectra of dyes **TTMS**, **TMS**, **TDS** and **TTS** in chloroform solvent

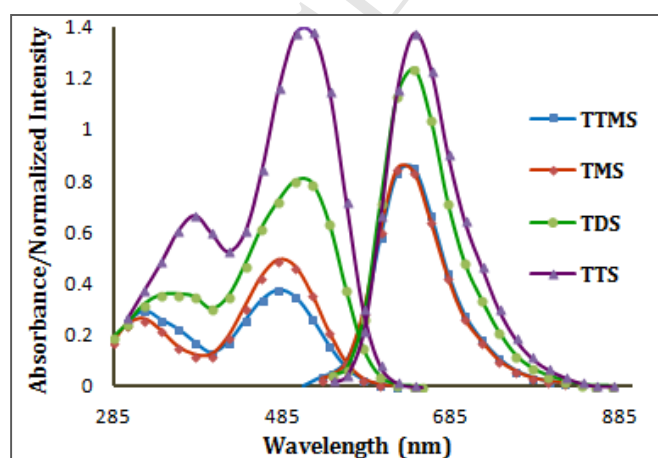
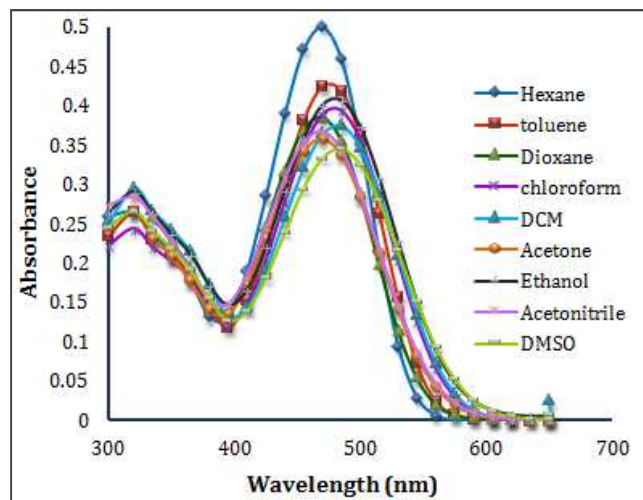
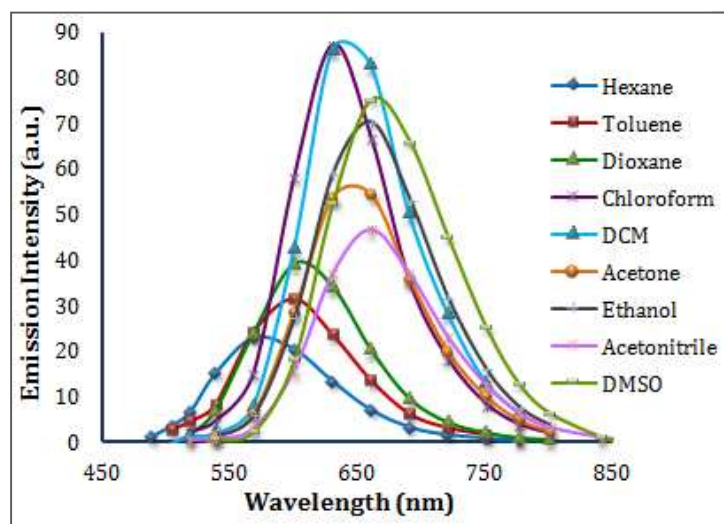


Fig. 3. Absorption spectra of dye TTMS in all solvents**Fig 4.** Emission spectra of dye TTMS in all solvent**Fig 5.** Normalized emission spectra of dye TTMS in all solvents

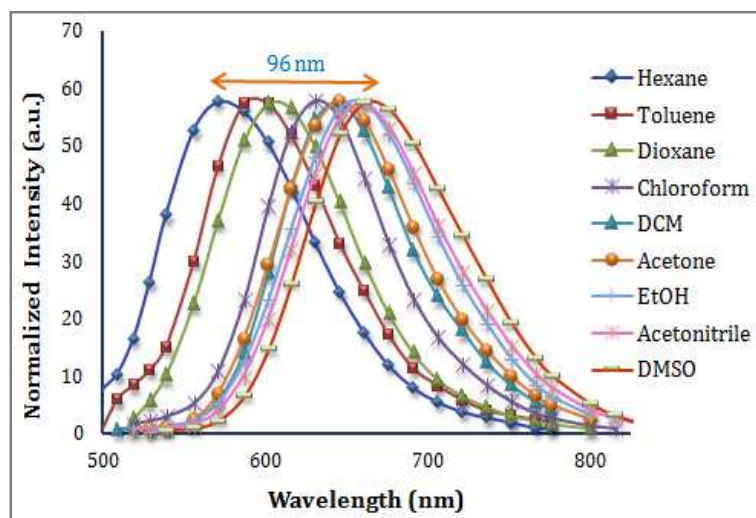


Fig. 6. Lipper-mataga solvent polarity graphs for all four dyes

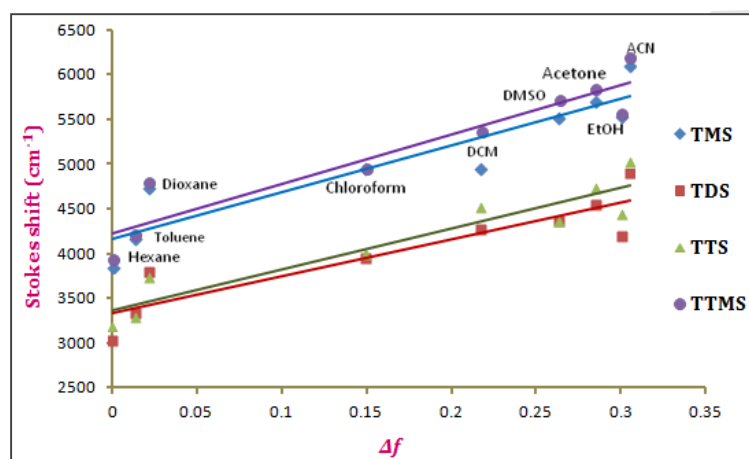


Fig. 7. Correlation between experimental and predicted emission wave number for TMS (a), TDS (b), TTS (c) and TTMS (d) by Catalan method.

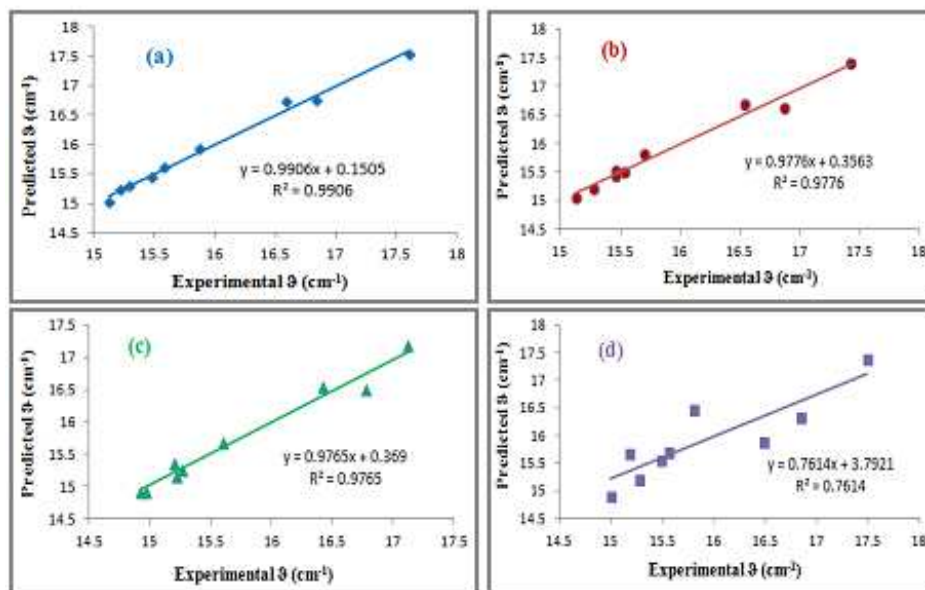


Fig. 8. Emission spectra of compound TMS, TTMS, TDS and TTS in all solvents. Designed line represents non-polar solvents while plane line represents polar solvents

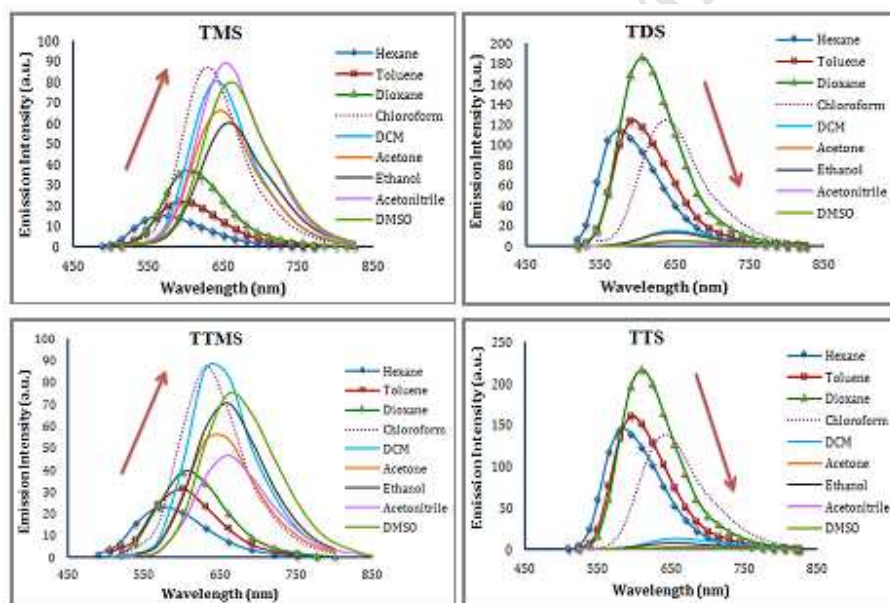
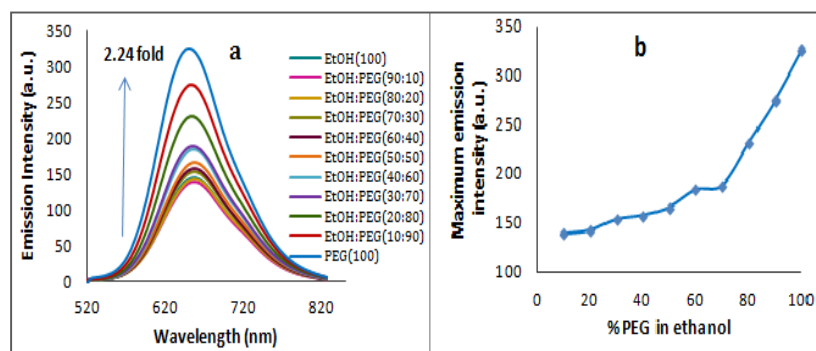
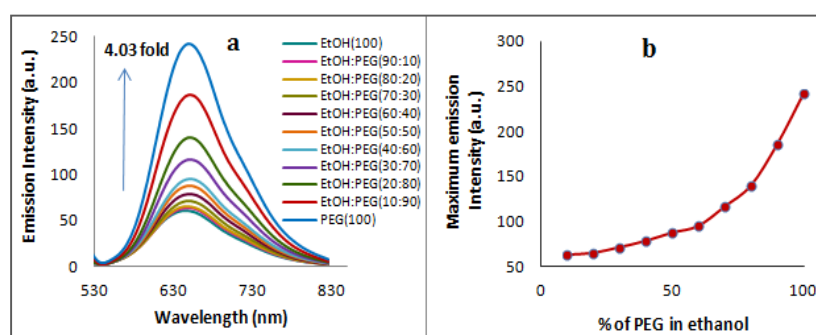


Fig. 9. Emission spectra of compound TMS (I), TDS (II), TTS (III) and TTMS (IV) in mixture of ethanol and PEG 400

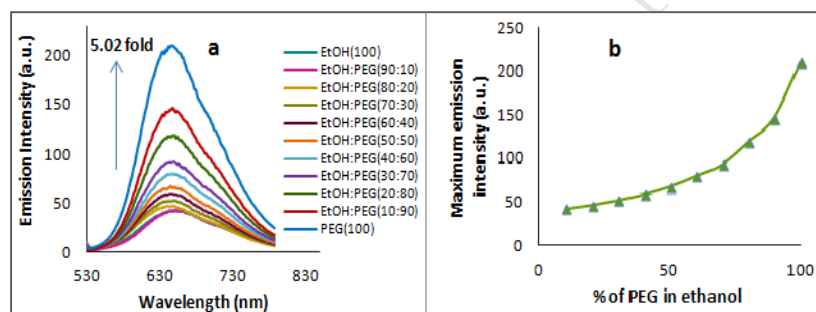
(I)



(II)



(III)



(IV)

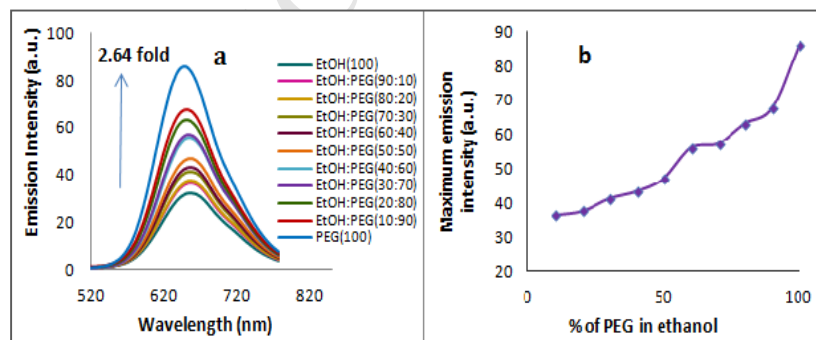


Fig.10 Cyclic voltammograms of dye TMS, TDS, TTS and TTMS in DCM at room temperature

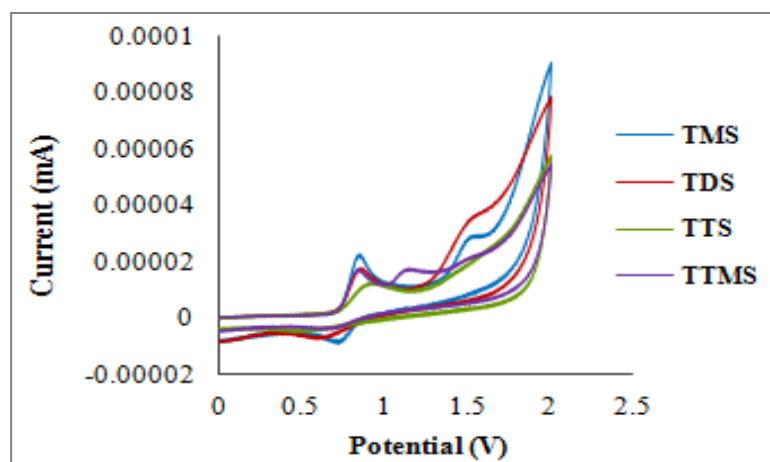


Fig.11: Comparative photophysical properties of Comp 1 (reported dye), TMS and TTMS dye

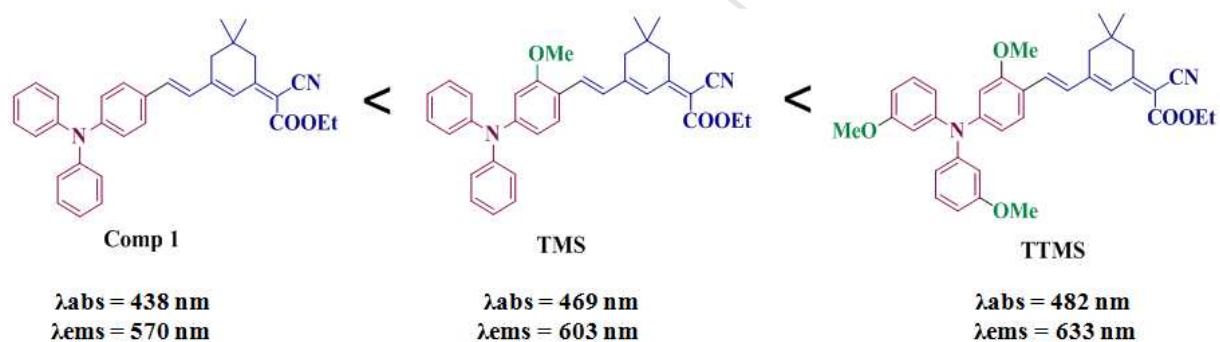


Fig. 12. HOMO-LUMO FMO diagrams of dye TMS, TTMS, TDS and TTS in gas phase at ground state

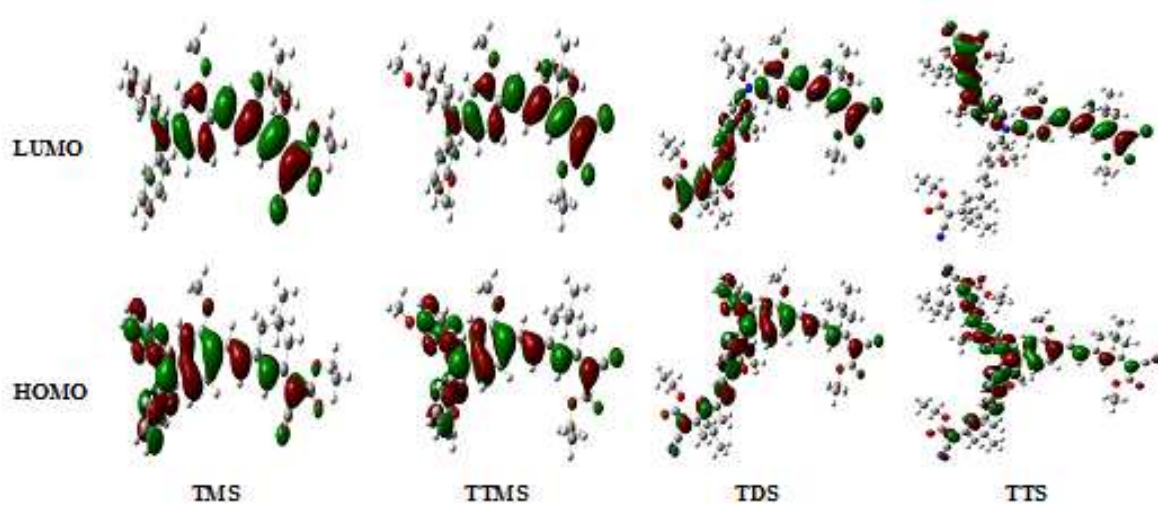
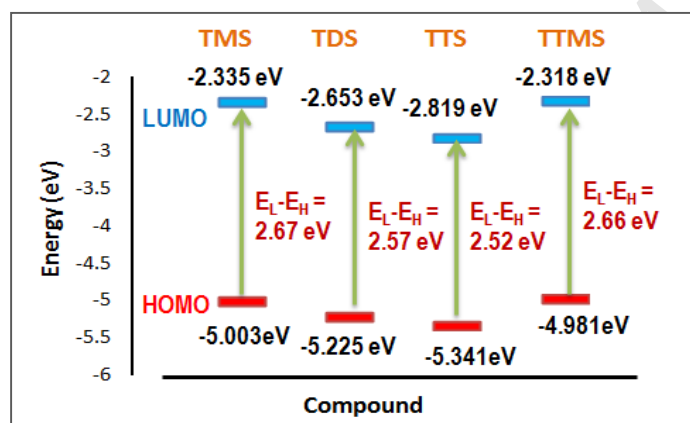


Fig. 13. HOMO-LUMO energy gaps of dyes TMS, TDS, TTS and TTMS in gas phase



Highlights

- Novel strategy is used for the synthesis of triphenylamine-isophorone styryl dyes.
- Tri-formylation of triphenylamine easily occurred due to the methoxy support.
- The dyes are categorized into ICT and TICT dyes as per their viscosity sensitivity.
- Red shifted absorptions-emissions are observed due to the auxiliary methoxy donors.